Derivation of the low-T phase diagram of LiHo$_x$Y$_{1-x}$F$_4$: A dipolar quantum Ising magnet

M. Schechter[1] and P. C. E. Stamp[1,2]

[1]*Department of Physics and Astronomy, University of British Columbia, Vancouver, British Columbia, Canada V6T 1Z1*

[2]*Pacific Institute for Theoretical Physics, University of British Columbia, Vancouver, British Columbia, Canada V6T 1Z1*

The LiHo$_x$Y$_{1-x}$F$_4$ compound is widely considered to be the archetypal dipolar quantum Ising system, with longitudinal dipolar interactions V_{ij}^{zz} between Ho spins $\{i,j\}$ competing with transverse field–induced tunneling, to give a $T=0$ quantum phase transition. By varying the Ho concentration x, the typical strength V_0 of V_{ij}^{zz} can be varied over many orders of magnitude, and so can the transverse field $H_\perp$. A new effective Hamiltonian is derived, starting from the electronuclear degrees of freedom, which is valid at low and intermediate temperatures. For any such dipolar quantum Ising system, the hyperfine interaction will dominate the physics at low temperatures, even if its strength $A_0 < V_0$: One must therefore go beyond an electronic transverse field quantum Ising model. We derive the full phase diagram of this system, including all nuclear levels, as a function of transverse field $H_\perp$, temperature T, and dipole concentration x. For LiHo$_x$Y$_{1-x}$F$_4$ we predict a re-entrant critical field as a function of x. We also predict the phase diagram for $x=0.045$ and the behavior of the system in magnetic-resonance and muon-spin-relaxation experiments.

I. INTRODUCTION

A. Transverse field quantum Ising model for LiHo$_x$Y$_{1-x}$F$_4$

For at least a decade the LiHo$_x$Y$_{1-x}$F$_4$ compound has been considered to be an ideal experimental realization of the well-known three-dimensional transverse field quantum Ising model (TFQIM). According to this view, at temperatures well below an anisotropy energy Ω_0, it is described by the Hamiltonian

$$H = -\sum_{i,j} V_{ij}^{zz} \tau_i^z \tau_j^z - \Delta_0 \sum_i \tau_i^x, \qquad (1)$$

where $\vec{\tau}_j$ is a Pauli vector describing a two-level effective electronic spin at spatial position $\mathbf{r} = \mathbf{r}_j$. V_{ij}^{zz} is a longitudinal interspin interaction, with nearest-neighbor strength U_0, which, depending on the dilution x, can have either a ferromagnetic (FM) or a frustrating character. The "transverse field" term $\Delta_0 \Sigma_i \tau_i^x$ is controllable externally (usually by applying a transverse magnetic field). The most distinctive feature of TFQI model (1), which is central to the whole field, is the competition between V_0, which tries to order the system, and Δ_0, which causes quantum fluctuations out of the ordered state. At $T=0$ one expects a quantum phase transition between ordered and quantum disordered states when $\Delta_0/V_0 \sim 1$; this is probably the simplest theoretical example of a quantum phase transition. The apparent confirmation of this "quantum critical" picture for LiHo$_x$Y$_{1-x}$F$_4$ has lent considerable importance to the experiments on this system.

The main arguments in favor of this picture for LiHo$_x$Y$_{1-x}$F$_4$ are as follows:

(i) The strong crystal-field Ho single-ion anisotropy yields an Ising doublet ground state, with a crystal-field Hamiltonian yielding an appreciable Δ_0 at small $H_\perp$. The dominant inter-Ho spin-spin interaction is dipolar, with strength $V_0(x) = \Sigma_j \langle V_{ij}^{zz} \rangle \sim \alpha x$, with $\alpha \sim 1$ in kelvins. Thus when $x=1$ one expects a dipolar-ordered FM phase below ~ 1 K, which is observed. It exhibits both classical and quantum phase transitions to the paramagnetic (PM) phase.[1]

(ii) In LiHo$_x$Y$_{1-x}$F$_4$ the magnetic Ho ions and the nonmagnetic Y ions have very similar atomic volumes. Dilution of Ho by Y is then possible with negligible distortion of the lattice. This dilution weakens the interactions and introduces randomness and frustration. Very different physical regimes can then be studied;[2,3] see Fig. 1 of Ref. 2. In particular, one expects a low-T spin-glass (SG) phase at small x, below a transition temperature $T_c \sim \alpha x$. At $x=0.167$ a SG phase is found[4,5] at low T and $H_\perp = 0$, with a crossover to the PM phase at higher T and $H_\perp$. At $x=0.44$ the tunneling of domain walls in the FM phase was found[6] and differences between quantum and classical annealing protocols were observed.[7] At $x=0.045$ the system shows a peculiar narrowing of the spin-fluctuation spectral width as the temperature is decreased,[8] described as "anti-SG" behavior.

(iii) For extreme dilution one expects single Ho ion behavior. In experiments at $x=0.002$, hysteresis loops of the magnetization due to single spin tunneling are observed.[9] (Cotunneling of pairs of spins was also observed at $x=0.002$, showing that interaction effects cannot be neglected even at this dilution.[10,11])

Thus, according to these arguments, a TFQI model such as Eq. (1) should describe LiHo$_x$Y$_{1-x}$F$_4$ for all x provided kT, $\mu_B H_\perp \ll \Omega_0$. As such, LiHo$_xY_{1-x}F_4$ should be a model system for all dipolar magnets. However we argue in this paper that the LiHo$_x$Y$_{1-x}$F$_4$ system (and, by implication, many other dipolar magnets) need to be described in a quite different way. There are two main problems with the simple TFQI picture, both noted and analyzed in Ref. 12. These are:

(a) *Hyperfine interactions*: The on-site Ho hyperfine interaction A_0 is not small. In fact, even at $x=1$, $A_0 \sim V_0$; and for $x \ll 1$, the hyperfine interaction is overwhelmingly dominant. A few experimental papers have heeded this point, remarking: (i) that even the $x=1$ phase diagram, near the $T=0$ FM-PM transition, is modified by the hyperfine interaction;[1] and (ii) that the nuclear-spin bath, considered now as a quantum environment,[13] should strongly affect the Ho spin dynamics near this quantum critical point.[14,15] However we shall show here that the effect of nuclear spins on dipolar

magnets is much more profound than this, *even when the hyperfine interaction is quite weak.* This very surprising result means that one must reconsider the application of the TFQI Hamiltonian to a large variety of systems, hitherto analyzed without reference to the hyperfine couplings.

(b) *Transverse dipolar interactions:* When $x \neq 1$ these interactions add a quite large contribution to the transverse field. To quantitatively understand the phase diagram, one then needs to include them[12,16] (see also Ref. 17), both in the SG and in the FM regimes.[12,16,18–20]

B. Electronuclear quantum Ising model for dipolar Ising magnets

To properly treat the physics of quantum Ising systems, we have to recognize that the use of a simple parameter $\Delta_0(H_\perp)$, introduced a long time ago by experimentalists as a convenient way of defining an effective transverse field acting on the Ising spins, is actually misleading. Because of the nuclear spins, the true effective transverse field in a quantum Ising system is very different from Δ_0. Moreover it depends on the actual nuclear-spin state of the system.

In what follows we will derive a theoretical framework with the nuclear spins included from the beginning. The system is described at low energies in terms of "electronuclear" complexes which interact via renormalized dipolar interactions. In its general form [see Eq. (3)], this "electronuclear quantum Ising" (ENQI) Hamiltonian includes all the nuclear-spin levels. However at very low T or for small x, we can use a much simpler Hamiltonian referring only to the lowest electronuclear doublet, and this takes the form

$$H = -\sum_{i,j} \widetilde{V}_{ij}^{zz}(H_\perp) s_i^z s_j^z - \widetilde{\Delta}(H_\perp) \sum_i s_i^x, \qquad (2)$$

where now $\hat{s}_j$ operates only on the single electronuclear doublet involving the nuclear states with $I_z = \pm I$. Now this simplified model looks like the standard TFQI model in Eq. (1), but it behaves very differently: Both $\widetilde{V}_{ij}^{zz}(H_\perp)$ and $\widetilde{\Delta}(H_\perp)$ are renormalized from their original values in Eq. (1), and they depend strongly on $H_\perp$. [In the case of $\widetilde{\Delta}(H_\perp)$, this dependence is radically different from that in the original parameter $\Delta_0(H_\perp)$.] The strength and behavior with field of these variations depend crucially on the strength A_0 of the hyperfine interaction. Moreover, as noted above, we must use this ENQI model at low T even when the hyperfine coupling $A_0 \ll V_0$, which is more typical for a general anisotropic magnet.

More generally, when kT is not small compared to the splitting between nuclear levels, we must define a set of $2I+1$ electronuclear "pseudospins" (each of which are spin-1/2 doublets) labeled by quantum numbers $m = I, I-1, \ldots, -I$, an occupation number n_{im} for the occupation of a given pseudospin on site i, and a set of pseudospin operators $\hat{s}_{im}$ and pseudospin energies ϵ_m. We then have the general ENQI Hamiltonian

$$H = -\sum_{i,j,m,m'} \widetilde{V}_{ij,m,m'}^{zz}(H_\perp) n_{im} n_{jm'} s_{im}^z s_{jm'}^z$$
$$- \sum_{i,m} n_{im} [\epsilon_m + \widetilde{\Delta}_m(H_\perp) s_{im}^x], \qquad (3)$$

where the $\widetilde{V}_{ij,mm'}^{zz}(H_\perp)$ represent interactions between pseudospins m, m' on different sites i, j and the transition matrices $\widetilde{\Delta}_m$ operate only on individual pseudospins, i.e., within the space of each electronuclear doublet on a given site. We can think of a set of $2I+1$–independent quantum Ising systems, each with a different transverse field $\widetilde{\Delta}_m$, which however can interact via the longitudinal fields $\widetilde{V}_{ij,mm'}^{zz}(H_\perp)$.

In disordered dipolar-coupled spin systems, one must also add a term which describes the random transverse couplings in the system. Its detailed form is given in Sec. III, and its quantitative effects are discussed in Sec. IV.

In this paper we concentrate on the $\text{LiHo}_x\text{Y}_{1-x}\text{F}_4$ system, for which precise results and experimental predictions can be established for the phase diagram, so it can be used as a test case. The effective Hamiltonian is strictly applicable to systems where $A_0, V_0 \ll \Omega_0$, in the regime where $T, \mu_B H_\perp \ll \Omega_0$. This approach enables: (i) illumination of the relevant physics of the $\text{LiHo}_x\text{Y}_{1-x}\text{F}_4$ system; (ii) generalization to other systems, e.g., systems in which $A_0 \ll V_0$ (see Sec. IV); and (iii) construction of a framework for the treatment of dynamical properties. However, in the $\text{LiHo}_x\text{Y}_{1-x}\text{F}_4$ system the condition $A_0, V_0 \ll \Omega_0$ is not that well satisfied. Moreover, while the condition $T, \mu_B H_\perp \ll \Omega_0$ is satisfied in the whole relevant phase diagram at low x, it is not satisfied near criticality at large concentrations. For this reason and since single-ion properties dictate much of the physics in the $\text{LiHo}_x\text{Y}_{1-x}\text{F}_4$ system, we also use exact diagonalization of the Ho electronuclear-spin states. This enables us to give quantitative predictions regarding the single-ion characteristics and, with the use of mean-field approximation, to predict the form of the phase diagram for all x.

To the best of our knowledge, most of the results here have not been published before. We analyze in detail the form of the electronuclear states of the single Ho ion as function of $H_\perp$ and its consequences in terms of entanglement entropy and magnetic-resonance experiments. We show that the peculiar crystal-field Hamiltonian of $\text{LiHo}_x\text{Y}_{1-x}\text{F}_4$ results in a well-defined Ising system even at high transverse fields (where Ising symmetry is usually destroyed). We obtain a general effective Hamiltonian valid for thermodynamic properties, incorporating all 16 low-energy states and therefore generalizing the treatment in Ref. 12 to the regime $A_0 < T \ll \Omega_0$. We give a discussion of the phase diagram for general concentration x, temperature T, transverse field $H_\perp$, and hyperfine coupling A_0. With relevance to general magnetic systems, we show that the hyperfine interactions dominate the physics at low T even when $A_0 \ll V_0$. By comparing the phase diagrams at $x = 0.045$ and $x = 0.167$, we predict a novel re-entrance of the crossover transverse field between the quasi-SG and PM phases at low T as a function of x, resulting from the interplay between the hyperfine and off-diagonal dipolar interactions. We then give give our own

view on the unsolved question of the nature of the low-T phase at $x=0.045$. Finally, we discuss some other experimental consequences and predictions of our theory.

The paper is organized as follows: In Sec. II the various terms in the microscopic Hamiltonian for LiHo$_x$Y$_{1-x}$F$_4$ are introduced and quantified and single-ion properties are analyzed. In Sec. III the full low-energy effective Hamiltonian is derived, including the transverse hyperfine interactions and the off-diagonal terms of the dipolar interaction. In Sec. IV we obtain the phase diagram of the LiHo$_x$Y$_{1-x}$F$_4$ system at different dilutions. We obtain quantitative agreement with the experimental phase diagram at $x=0.167$, make predictions regarding the phase diagram at $x=0.045$, and discuss the nature of the low-temperature phase. In Sec. V we suggest experiments that can directly check our theory, and in Sec. VI we state our conclusions. Some details regarding the derivation of the effective Hamiltonian and the calculation of the phase diagram in mean field are deferred to appendices.

II. INTERACTIONS IN THE LiHo$_x$Y$_{1-x}$F$_4$ SYSTEM

In this section we give the quantitative form of the LiHo$_x$Y$_{1-x}$F$_4$ Hamiltonian, which is a sum of crystal-field,[9,21] Zeeman, inter-Ho, and hyperfine interaction terms:

$$H = H_{cf} + H_Z + H_{int} + H_{hyp}. \tag{4}$$

Note that we have dropped: (i) the spin-phonon interaction, important for spin relaxation;[9,10,22] (ii) hyperfine interactions between the Ho ion and other nuclear species (F, Li) as well as with Ho nuclei on nearby sites; and (iii) the nuclear Zeeman couplings. None of these terms have an appreciable effect on the phase diagram of LiHo$_x$Y$_{1-x}$F$_4$. Note however that they will be crucial for the low-T Ho spin dynamics, since even very small hyperfine terms can strongly affect relaxation dynamics and decoherence in the low-T quantum regime,[23,24] where phonon relaxation is also important in strong transverse fields.[23,25]

A. TFQIM terms

Let us first consider the terms which feed directly into TFQIM Hamiltonian (1), i.e., the terms H_{cf}, H_Z, and H_{int}. For LiHo$_x$Y$_{1-x}$F$_4$ these are given in turn by:

(i) The "crystal-field" term H_{cf} includes the single-ion crystal-field and spin-orbit terms.[9,21] Because of the very strong spin-orbit coupling, J is a good quantum number for the Ho ion with $J=8$. A crystal-field term of the form ($J_+^4 + J_-^4$) strongly mixes states with J_z differing by ± 4,[9,26] and a strong J_z^2 term severely distorts the level spacing. There are other terms as well. For computations in this paper we will use a form written in terms of the usual Stevens operators as[14,21]

$$H_{cf} = \sum_{l=2,4,6} B_l^0 O_l^0 + B_6^4 O_6^4(S) + \sum_{l=4,6} B_l^4 O_l^4(C), \tag{5}$$

with values assumed to be[21]
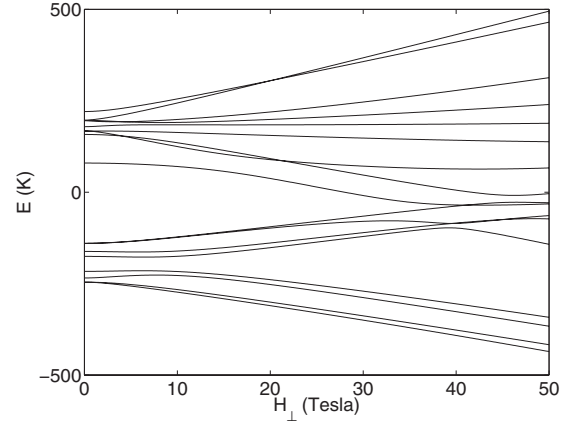
$$B_2^0 = -0.696, \quad B_4^0 = 4.06 \times 10^{-3},$$

FIG. 1. Energy of the 17 electronic states of a single Ho ion in LiHo$_x$Y$_{1-x}$F$_4$, ignoring all inter-Ho interactions, as a function of transverse field $H_\perp$. The Ising-type character is well maintained until $H_\perp \approx 20$ T.

$$B_6^0 = 4.64 \times 10^{-6}, \quad B_4^4(C) = 4.18 \times 10^{-2},$$

$$B_6^4(C) = 8.12 \times 10^{-4}, \quad B_6^4(S) = 1.137 \times 10^{-4}, \tag{6}$$

from which we see that the $O_6^4(C)$ term also has a nontrivial effect, bringing in a $J_z^2(J_+^4 + J_-^4)$ term. (Note that to properly judge the relative importance of coefficients B_l^m and $B_{l'}^m$ with $l \neq l'$, we should directly compare $J^l B_l^m$ and $J^{l'} B_{l'}^m$, *not* B_l^m and $B_{l'}^m$.)

The ground state is an Ising doublet, with states denoted here by $|\uparrow\rangle$ and $|\downarrow\rangle$, which mix states with $J_z = \pm 7, \pm 3, \mp 1, \mp 5$. The first excited state $|\Gamma_2^l\rangle$ is roughly $\Omega_0 = 10.5$ K above the ground-state doublet and is a mixture of $J_z = 6, 2, -2, -6$. The other 14 states are much higher in energy, and the total span of the $J=8$ manifold is roughly $\Omega_f = 500$ K.[26]

(ii) The Zeeman coupling to the Ho spins is given by the usual form

$$H_Z = -\sum_i g_J \mu_B \vec{H} \cdot \vec{J}_i, \tag{7}$$

with $g_J = 5/4$. We are particularly interested in the effect of a transverse field $H_\perp \ll \Omega_0/\mu_B$, which induces a coupling Δ_0 between the two Ising ground states in second-order perturbation theory via the state $|\Gamma_2^l\rangle$. Thus, for small fields $\Delta_0 \propto H_\perp^2$; by putting in the numbers, one finds

$$\Delta_0(H_\perp) \sim 9(\mu_B H_\perp)^2/\Omega_0 \approx 0.4T^2 \tag{8}$$

in kelvins (see, e.g., Figs. 1 and 2 of Ref. 21). At larger fields, $H_\perp \approx \Omega_0/\mu_B \approx 2$ T, perturbation theory breaks down, $|\Gamma_2^l\rangle$ mixes strongly with $|\uparrow\rangle$ and $|\downarrow\rangle$,[21] and Δ_0 is approximately linear in $H_\perp$. An important feature of LiHo$_x$Y$_{1-x}$F$_4$ is that $\Omega_f \gg \Omega_0$. Thus, the system stays Ising type even when $H_\perp > \Omega_0/\mu_B$, deep inside the PM regime (see Fig. 1). This contrasts with most other anisotropic dipolar systems, which are dominated by easy-axes terms, so that the same energy scale dictates the anisotropy and the quantum fluctuations,

and in the quantum phase transition regime $H_\perp \approx H_\perp^c$, there is no real Ising character.

(iii) The inter-Ho ion spin-spin interactions depend strongly on the Ho concentration x. They have the general form

$$H_{int} = -\sum_{ij} U_{ij}^{\alpha\beta} J_i^\alpha J_j^\beta. \tag{9}$$

Experiments[27] and theoretical analysis[21] both show that $U_{ij}^{\alpha\beta}$ is dominated by the dipolar interaction, i.e.,

$$U_{ij}^{\alpha\beta} = \frac{U_0 \mathcal{R}_{ij}^{\alpha\beta}}{J^2}, \tag{10a}$$

$$\mathcal{R}_{ij}^{\alpha\beta} = \mathcal{V}_c \frac{|\mathbf{r}_{ij}|^2 \delta_{\alpha\beta} - 3r_{ij}^\alpha r_{ij}^\beta}{|\mathbf{r}^{ij}|^5}. \tag{10b}$$

Here the strength of the nearest-neighbor dipole-dipole interactions between the spins $\mathbf{J}_i$, $\mathbf{J}_j$ is

$$U_0 = \frac{\mu_0}{4\pi} \frac{g_J^2 \mu_B^2 J^2}{\mathcal{V}_c}, \tag{11}$$

where $\mathcal{V}_c$ is the unit-cell volume. The unit-cell size is $(1,1,2.077)$ in units of $\tilde{a} = 5.175$ Å, with four Ho ions per unit cell when $x=1$, at positions $(0,0,0)$, $(0, a/2, c/4)$, $(a/2, a/2, -c/2)$, and $(a/2, 0, -c/4)$; and $\mathbf{r}_{ij} = \mathbf{r}_i - \mathbf{r}_j$. When $x < 1$ some of the Ho ions are substituted by Y ions, and the couplings acquire a random distribution, whose character depends strongly on x. The typical value $\bar{U}_0$ of the nearest-neighbor coupling then becomes roughly $\bar{U}_0 \sim xU_0$. For LiHo$_x$Y$_{1-x}$F$_4$, $U_0 \sim 0.3$ K. Note however that the energy V_0 characterizing the total effect of the longitudinal dipolar interactions is somewhat larger than $\bar{U}_0$, since as noted in Sec. I, $V_0(x) = \sum_j \langle V_{ij}^{zz} \rangle$. Thus the strength of V_0 depends on how the spins are arranged. It can be estimated from the ordering temperature, and typically $V_0/\bar{U}_0 \sim 3-5$. One can see departures from linearity in x. For example, in the diluted system, even for rather small x, close pairs and even triplets can dominate certain properties. There are also antiferromagnetic exchange interactions between the Ho ions, which for $x=1$ were measured to be about half of the nearest-neighbor dipolar interaction.[27] Therefore, the exchange interactions have little quantitative significance even for the undiluted LiHoF$_4$ (Ref. 21) and are completely negligible for $x \ll 1$.

If we now take these three terms and truncate the Ho ions to their lowest doublet, we get back the TFQIM in Eq. (1), which predicts a quantum phase transition for $x=1$ at a transverse field where $\Delta_0 \sim V_0$, i.e., at $H_\perp \approx 3$ T.[1,21] In fact the actual transition happens at $H_\perp^c(x=1) = 4.9$ T,[1,21] which is the first sign that there is something wrong with this naive picture. To see what is going on, we now have to include the hyperfine coupling.

B. Hyperfine interactions

The hyperfine coupling of a single Ho atom with its own $I=7/2$ nuclear spin gives the term
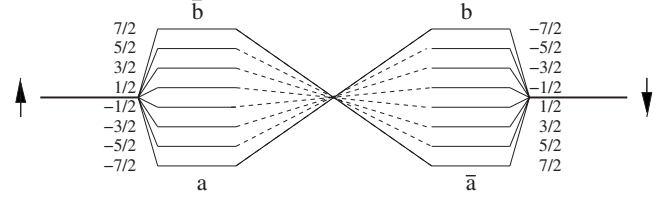

FIG. 2. Splitting of the electronic low-energy doublet ($\uparrow$ and $\downarrow$) by the longitudinal hyperfine interaction. The ground-state doublet states a and $\bar{a}$ have a definite and opposite nuclear spin, $\pm 7/2$. A transverse magnetic field $H_\perp$ couples states with the same nuclear spin, as shown by the dashed lines.

$$H_{hyp} = A_J \sum_i \vec{I}_i \cdot \vec{J}_i, \tag{12}$$

with $A_J = 0.039$ K.[9] Here we ignore quadrupolar terms as well as the hyperfine interactions to all other species (Li, F, and other Ho ions). Both are an order of magnitude smaller[28] and hardly influence the phase diagram.

At low energies, in the lowest doublet states $|\uparrow\rangle$, $|\downarrow\rangle$, the longitudinal hyperfine term $H_{hyp}^\parallel = A_J I^z J^z$ splits each electronic state into an eightfold multiplet of nearly equidistant levels, with separation of ~ 205 mK (Ref. 9) between adjacent levels. I.e., we can write

$$H_{hyp}^{zz} \sim \omega_0 \tau_z I_z, \tag{13}$$

where $\hat{\tau}$ operates on the electronic doublet and for LiHo$_x$Y$_{1-x}$F$_4$, $\omega_0 \sim 205$ mK. This corresponds to a spin moment $\langle J_z \rangle \sim 5\mu_B$ for the lowest doublet.

One can see without any reference to experiments on the phase diagram that the TFQI model cannot possibly be right at low transverse fields, using Fig. 2. The lowest-energy Ising doublet states a, $\bar{a}$ have a definite nuclear spin ($I_z = -7/2$ for $|\uparrow\rangle$ and $I_z = 7/2$ for $|\downarrow\rangle$) when $H_\perp = 0$. A transverse magnetic field couples $a \equiv |\uparrow, -7/2\rangle$ to $b \equiv |\downarrow, -7/2\rangle$ and $\bar{a} \equiv |\downarrow, 7/2\rangle$ to $\bar{b} \equiv |\uparrow, 7/2\rangle$. It cannot induce quantum fluctuations between the relevant Ising doublet ground states at all but can only renormalize their effective spin. Only the *transverse* hyperfine term $H_{hyp}^\perp = A_J(I^+ J^- + I^- J^+)/2$ can change I_z and allow transitions between the Ising doublet states. However this hardly operates if $\mu_B H_\perp \ll \Omega_0$.

Thus hyperfine interactions must be included in any truncation of the system to a low-energy Hamiltonian. Their general effect is to suppress quantum effects at low fields. We shall see that they are important even when $A_0 \ll V_0$. (Note that the simple argument above, showing the importance of the hyperfine effects, makes no reference to the strength of these interactions.)

C. Single Ho ion: Exact results for low energies

For $H_\perp \gg \Omega_0/(\mu_B \langle J_z \rangle)$, $H_{hyp}^\perp$ mixes appreciably electronuclear states with different values of I_z. This is best seen by performing an exact diagonalization of the full single Ho Hamiltonian $H = H_{cf} + H_Z + H_{hyp}$ in the 136 eigenfunction space (17 crystal field $\times$ 8 nuclear states). In Fig. 3 we plot the spectrum of the lowest 16 levels, corresponding to the electronic ground-state doublet, as a function of $H_\perp$. Most
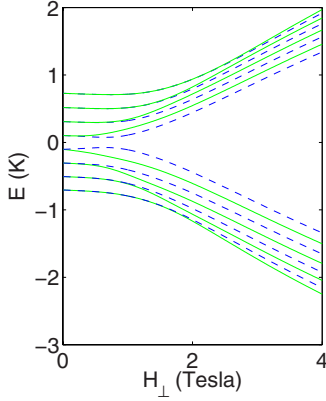
FIG. 3. (Color online) The 16 lowest electronuclear energy levels of LiHo$_x$Y$_{1-x}$F$_4$, plotted as a function of transverse magnetic field $H_\perp$. The zero of energy is defined by the (field-dependent) mean of levels 8 and 9. Symmetric/antisymmetric states are plotted as solid green/dashed blue lines.

generally, each of the 16 states can be written in the form $\sum_{M,m}\alpha_{Mm}|M,m\rangle$, where $M(m)$ denote the z component of the electronic (nuclear) spin. Plotted as solid lines are symmetric eigenstates, with $\alpha_{Mm}=\alpha_{-M-m}$, and as dashed lines are antisymmetric eigenstates, with $\alpha_{Mm}=-\alpha_{-M-m}$.

At low fields, the electronuclear entanglement is strong, and states are given, to a good approximation, by the form in Eq. (A3). One can then define the splitting between each pair of time-reversed states by $\widetilde{\Delta}_m$, which are plotted in Fig. 4. We find,[12] as we expect, that $\widetilde{\Delta}_{7/2}$ is small up to $H_\perp \approx 2$ T, at which point $\langle\uparrow|\mu_B H_\perp|\Gamma_2^l\rangle\approx\Omega_0$. $\widetilde{\Delta}_m$ increases more rapidly as $|m|$ decreases, simply because for smaller $|m|$, transitions between the two low-energy time-reversed states can be achieved by lower orders in perturbation theory in $H_{\text{hyp}}^\perp$. One then sees appreciable coupling at lower $H_\perp$. As $H_\perp$ continues to increase, $\widetilde{\Delta}_m$ increases rapidly and eventually saturates at a field $H_\perp^*(m)$. Note however that the spectrum in Fig. 3 is not
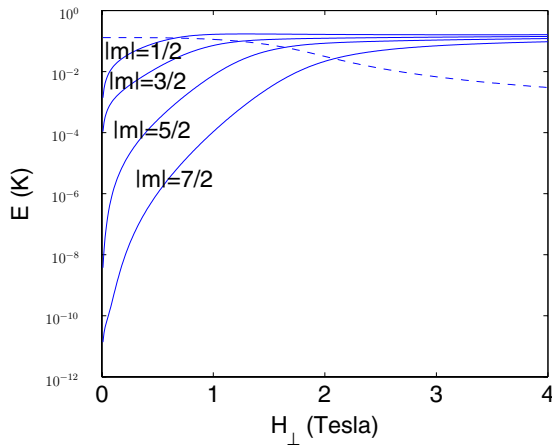

FIG. 4. (Color online) The quantum fluctuation amplitudes $\widetilde{\Delta}_m$ induced by $H_\perp$, plotted for $|m|=7/2$, $5/2$, $3/2$, $1/2$. The dashed line shows the effective dipolar interaction V_{ij}^{mm} at $x=0.167$ for $|m|=7/2$ (the low-T phase transition occurs when this interaction $\sim\widetilde{\Delta}_{7/2}$). Note how small is $\widetilde{\Delta}_m$ for large $|m|$ and small $H_\perp$.

symmetric. This is because tunneling between the lower pairs is allowed via the state $|\Gamma_2^l\rangle$ at energy Ω_0, whereas tunneling between the upper pairs must involve the higher excited states, at energy E_{CF} higher than the lowest states. Consider, e.g., the pairs $|\uparrow,-1/2\rangle$, $|\downarrow,1/2\rangle$ and $|\uparrow,1/2\rangle$, $|\downarrow,-1/2\rangle$. The first pair has a finite matrix element in second-order perturbation, $\langle\uparrow,-1/2|H_x J_x |\Gamma_2^l\rangle\langle\Gamma_2^l|I_x J_x|\downarrow,1/2\rangle$, which is first order in $H_\perp$, and gives a low-field splitting $\propto H_x I_x/\Omega_0$. The second pair has a term of similar form, which however passes via the states in the multiplet $J_z=8,4,0,-4,-8$. Thus it gives a low-field splitting $\propto H_x I_x/E_{\text{CF}}$, roughly an order of magnitude smaller.

For $H_\perp\gtrsim H_\perp^*(m)$ different values of m are well mixed, and the electron and nuclear spins get disentangled, and the spectrum separates to two groups of eights. For $H_\perp\gtrsim H_\perp^*(7/2)$ the eigenstates can be approximated by $|\psi_I\rangle|\psi_J\rangle$. The electronic state hybridizes strongly the level $|\Gamma_2^l\rangle$ with the ground-state doublet. The states in the bottom group are approximately symmetric with respect to the electronic degrees of freedom, i.e., they have $\alpha_{Mm}\approx\alpha_{-Mm}$, while the states in the upper group have $\alpha_{Mm}\approx-\alpha_{-Mm}$. In each group, states separate into pairs of symmetric and antisymmetric states, as noted above. For large $H_\perp$ the lower level of each pair has $\alpha_{Mm}\approx\alpha_{M-m}$ and the higher level has $\alpha_{Mm}\approx-\alpha_{M-m}$. Both the energy spectrum and the form of the eigenstates discussed above should be revealed in electromagnetic-resonance experiments. In Sec. V A 1 we give predictions for such possible experiments, and their relation to the calculated entanglement entropy.

III. LOW-T ENQI EFFECTIVE HAMILTONIAN

We now incorporate all the terms in Eq. (4), with all nuclear levels and the off-diagonal dipolar interactions, into the full ENQI model for the LiHo$_x$Y$_{1-x}$F$_4$ system, including all terms relevant to the phase diagram at energies >10 mK. We begin by dividing the original Hamiltonian [Eq. (4)] into the form

$$H = H_0 + H_1^{zz} + H_1^\perp, \tag{14}$$

where

$$H_0 = H_{\text{cf}} + H_{\text{hyp}}^{zz} + H_Z,$$

$$H_1^{zz} = U_{\text{dip}}^{zz},$$

$$H_1^\perp = H_{\text{hyp}}^\perp + U_{\text{dip}}^\perp \tag{15}$$

and where we have written the dipolar interaction in the form

$$U_{ij}^{\alpha\beta} = U_{ij}^{zz} + U_{ij}^\perp, \tag{16}$$

with a nondiagonal term

$$U_{ij}^\perp = \frac{U_0}{J^2}\mathcal{R}_{ij}^\perp = \frac{U_0}{J^2}[\mathcal{R}_{ij}^{\alpha\beta} - \mathcal{R}_{ij}^{zz}], \tag{17}$$

where $\mathcal{R}_{ij}^{\alpha\beta}$ was defined in Eq. (10b).

In Appendix A we derive a low-energy effective Hamiltonian valid for $T\ll\Omega_0$, $\mu_B H_\perp\ll\Omega_0$. We do this in three

steps. We first derive the effective Hamiltonian for $H = H_0 + H_1^{zz}$, including Ising interactions terms only, and obtain Eq. (A13). We then add $H_{\text{hyp}}^{\perp}$, which introduces a quantum term and obtain Eq. (A22). We finally include $U_{\text{dip}}^{\perp}$, which introduces an effective random field,[16] and an enhancement of the effective transverse field.[12] As a final low-T effective Hamiltonian for the LiHo$_x$Y$_{1-x}$F$_4$ system, we obtain

$$H_{\text{eff}} = - \sum_{i,j,m,m'} \widetilde{V}_{im,jm'}^{zz}(\widetilde{H}_i^{\perp}, \widetilde{H}_j^{\perp}) n_{im} n_{jm'} s_{im}^z s_{jm'}^z$$
$$- \sum_{i,m} n_{im} [\epsilon_m + \widetilde{\Delta}_m(\widetilde{H}_i^{\perp}) s_{im}^x] + \sum_i \gamma_i^{\tilde{z}}(H_{\perp}) \sum_m n_{i,m} s_{im}^z. \tag{18}$$

Here $\widetilde{\Delta}_m$ are the effective transverse fields acting on time-reversed states with a given $|m|$, as defined in Eq. (A10) (see Fig. 4), and $\gamma_i^{\tilde{z}}$ is an effective random field, defined in Eq. (A29). We note explicitly the dependence of the interactions and the effective transverse fields and random field on the site-dependent total transverse field $\widetilde{H}_i^{\perp}$ [Eq. (A30)].

In the low-T limit $kT \ll \omega_0$ and for $H_{\perp} < H_{\perp}^*(7/2)$, we obtain

$$H = - \sum_{i,j} \widetilde{V}_{ij}^{zz}(\widetilde{H}_i^{\perp}, \widetilde{H}_j^{\perp}) s_i^z s_j^z - \sum_i \widetilde{\Delta}(\widetilde{H}_i^{\perp}) s_i^x + \sum_i \gamma_i^{\tilde{z}}(H_{\perp}) s_i^z. \tag{19}$$

This Hamiltonian applies for any $x < 1$, irrespective of what thermodynamic phase results from it. Thus in LiHo$_x$Y$_{1-x}$F$_4$ it is valid for both the SG and FM regimes (the x dependence enters in the interaction terms and in the effective fields). Note that $\widetilde{\Delta}$ and $\gamma_i^{\tilde{z}}$ have very different dependences on $H_{\perp}$ and dilution x. Thus, in the FM phase $\widetilde{\Delta}$ and $\gamma_i^{\tilde{z}}$ are independently tunable, by changing x and $H_{\perp}$.[20] In LiHo$_x$Y$_{1-x}$F$_4$ one may thereby realize both the quantum and the classical random-field Ising models in a FM system (see the theoretical prediction in Ref. 20 and the experimental realization in Ref. 29).

We emphasize the essential role played here by the nuclear spins. They block quantum fluctuations. This is especially important for the LiHo$_x$Y$_{1-x}$F$_4$ system, whose peculiar crystal-field Hamiltonian allows electronic tunneling at second order in $H_{\perp}$. If we drop the nuclear spins, we can get erroneous results (e.g., that the effective random field must come at the expense of appreciable quantum fluctuations[18]). For some purposes one can circumvent a proper treatment of the hyperfine interactions by considering a simplified crystal-field Hamiltonian[16,19,20] (see also Ref. 30), where tunneling between the electronic spins is in high-order perturbation. This gives the correct effective random field and the re-entrance of the crossover $H_{\perp}$ as a function of dilution (see Sec. IV C). However, for other purposes a proper treatment of the hyperfine interactions is essential—e.g., for the temperature and field dependence of the phase diagram (see Sec. IV) and for all of the dynamic properties.

IV. MEAN-FIELD TREATMENT OF THE PHASE DIAGRAM

The phase diagram of quantum Ising systems such as LiHo$_x$Y$_{1-x}$F$_4$ has been the object of extensive study for over three decades. It was realized early on that strong hyperfine interactions might be important.[31] In the case of LiHo$_x$Y$_{1-x}$F$_4$, for $x=1$ the phase diagram was calculated in mean field,[1] including the longitudinal hyperfine interactions. This gave an enhancement of the critical transverse field at low temperatures.

In this section we analyze the phase diagram of the LiHo$_x$Y$_{1-x}$F$_4$ system in various dilutions, where disorder effects have to be accounted for. We first discuss the phase diagram of a model Hamiltonian, including first the longitudinal dipolar and hyperfine interactions and then adding the transverse hyperfine interaction. Using this model, we make predictions for the behaviors of the phase diagram and of the magnetization of a general anisotropic dipolar system where the conditions A_0, $V_0 \ll \Omega_0$ are well satisfied for an arbitrary ratio of A_0/V_0. This analysis also pinpoints the basic physics dictating the phase diagram in the LiHo$_x$Y$_{1-x}$F$_4$ system. However, in the LiHo$_x$Y$_{1-x}$F$_4$ system the condition $A_0 \ll \Omega_0$ is not that well maintained. To solve for the phase diagram of the LiHo$_x$Y$_{1-x}$F$_4$ system, we use exact diagonalization of the single Ho ion, a mean-field approximation for the inter-Ho interactions, and we take into account the enhancement of the effective transverse field by the transverse dipolar terms. We shall see that this then gives very accurate results for the phase lines for LiHo$_x$Y$_{1-x}$F$_4$ when $x=0.167$, and we make predictions for $x=0.045$.

Finally, we discuss the nature of the phases at low T; this is currently rather controversial. The hyperfine interactions again play a central role in reducing quantum fluctuations and slowing the relaxation of the system to equilibrium in the low-T quantum regime. At finite transverse field we discuss the effect of the effective longitudinal random field, emerging from the applied transverse field.

A. Classical Ising limit

As shown above, if $H_{\perp}$ is small, the transverse hyperfine interactions play a minor role (the $\widetilde{\Delta}_m$ are small), and the only effect of the longitudinal hyperfine interactions is to give a rather strong renormalization of the longitudinal dipolar interaction between the Ising doublet spins $\tau_j^{\tilde{z}}$. The problem in this Ising limit (neglecting the transverse terms) was studied previously[32] but only for $x=1$. We give a treatment here for all dilutions, and we also assume that A_0 is arbitrary. Surprisingly, the hyperfine interactions cannot be neglected even when $A_0 \ll V_0$.

1. Strong hyperfine interactions

When $A_0 > V_0$ and $kT < \omega_0$, the relevant Hilbert space comprises the lowest two electronuclear Ising-type levels, and we consider Hamiltonian (A2), which reduces to the classical Ising Hamiltonian $H_{\text{eff}}^{\parallel}$ given in Eq. (A9). The only
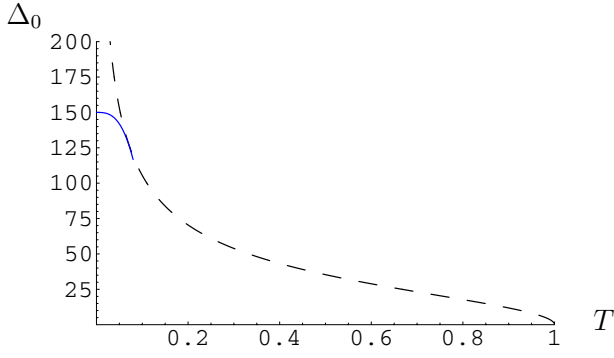
FIG. 5. (Color online) Plot of the phase line separating the ordered and the PM phases for model ($A2$) in the regime where $A_0 \gg V_0$, assuming $V_0 = 1$, $A_0 = 35$, and $\Omega_0 = 100$ in arbitrary units. The dashed line shows Eq. (20), plotted neglecting transverse hyperfine interactions. We see that Δ_c diverges as $T \to 0$. The blue solid line describes the deviation from the classical Ising model at high transverse fields, where the transverse hyperfine interaction are significant, giving a quantum phase transition (QPT) at $\Delta_0 \approx \Omega_0$ (see Sec. IV B).

effect of $H_\perp$ is to renormalize V_{ij}^{zz} to $\widetilde{V}_{ij}^{zz} = \eta^2 V_{ij}^{zz}$. We can then immediately deduce the whole phase diagram of the system. Since η is a function only of Δ_0/A_0 [see Eq. ($A7$)], we can write all expressions for the phase diagram in terms of Δ_0 instead of the actual transverse field $H_\perp$. The transition line as a function of Δ_0 is shown in Fig. 5 for $A_0 \gg V_0$ (i.e., for $x \ll 1$ in the LiHo$_x$Y$_{1-x}$F$_4$ system). This diagram simply depicts the relation[12]

$$T_c(\Delta_0) = \eta(\Delta_0)^2 T_c(0).$$ (20)

If we now define $\epsilon \equiv (T_c - T)/T_c$, one finds that for Δ_0/A_0, $\epsilon \ll 1$ (i.e., small $H_\perp$ and $T \sim T_c$), the phase transition line $\Delta_c(T)$ obeys the relation

$$\Delta_c = A_0\sqrt{\epsilon}.$$ (21)

At $T = T_c/2$ one finds that $\Delta_c \approx A_0$. When $\Delta_0/A_0 \gg 1$ there is still a finite remnant polarization of the spin and an ordered state at $T = 0$; the transition line obeys the relation $\Delta_c = A_0\sqrt{(V_0/T)}$. This is quite different from TFQI model (1), where for $\Delta_0 > V_0$ the system becomes a paramagnet and a $T = 0$ quantum critical point is observed.

2. Renormalized Ising model for arbitrary A_0/V_0

We now relax the condition $V_0 \ll A_0$, so that all hyperfine levels have to be included (however we still assume that nuclear-spin flips are blocked). For this case one can treat Hamiltonian ($A1$) using mean-field theory. It then reduces to the mean-field effective Hamiltonian

$$H_{MF} = \sum_i (hI_i^z - H_i^z)\tau_i^z - \sum_i \Delta_0 \tau_i^x,$$ (22)

where the site-dependent mean field is

$$H_i^z = \sum_j V_{ij}^{zz}\langle \tau_j^z \rangle$$ (23)

and $h \equiv \omega_0$.

Since Eq. ($A1$) is equivalent to classical Ising Hamiltonian ($A13$), mean-field Hamiltonian (22) is equivalent to the mean-field version of Eq. ($A13$), given by

$$H_{MF}^\| = \sum_{im} n_{im}(\epsilon_{im} + E_{im}\hat{s}_{im}),$$ (24)

where now the mean field is

$$E_{im} = \sum_{jm'} n_{jm'}\widetilde{V}_{im,jm'}^{zz}\langle \hat{s}_{jm'}^z \rangle.$$ (25)

The mean-field theory in form (22) was solved some time ago[32] for the homogeneous case (where $\langle \tau_j^z \rangle$ is independent of j; i.e., the mean field is the same at all sites) and applied to the FM LiHoF$_4$ system (i.e., when $x = 1$).

In this section we extend this mean-field approach to cover all values of x, including the SG regime, by allowing the local mean field to vary from site to site. In order to allow easy comparison with the previous work,[32] we do this starting from the Hamiltonian in form (22) rather than form (24). An explicit derivation, given in Appendix B, results in the self-consistent equation

$$1 = \frac{\sum_m \frac{\Delta_0^2 V_0}{(h^2 m^2 + \Delta_0^2)^{3/2}}\sinh(\beta\sqrt{h^2 m^2 + \Delta_0^2}) + \frac{\beta V_0 h^2 m^2}{h^2 m^2 + \Delta_0^2}\cosh(\beta\sqrt{h^2 m^2 + \Delta_0^2})}{\sum_m \cosh(\beta\sqrt{h^2 m^2 + \Delta_0^2})}.$$ (26)

When $A_0 \gg V_0$ the solution of this equation reproduces the results in Sec. IV A and in particular the phase diagram in Fig. 5. Let us now consider the regime $V_0 \gg A_0$. Expanding Eq. (26) in small Δ_0, one obtains the following behavior of the transition line $\Delta_c(T)$ near $T_c(0)$:

$$\Delta_c(\epsilon) = V_0\sqrt{\epsilon},$$ (27)

where $\epsilon \equiv (T_c - T)/T_c$. Because the dipolar interaction now dominates, the results of the TFQI model are reproduced near T_c; and at $T_c/2$ we find $\Delta_c \approx V_0$. Surprisingly, however, the hyperfine interaction, although small, dictates the physics
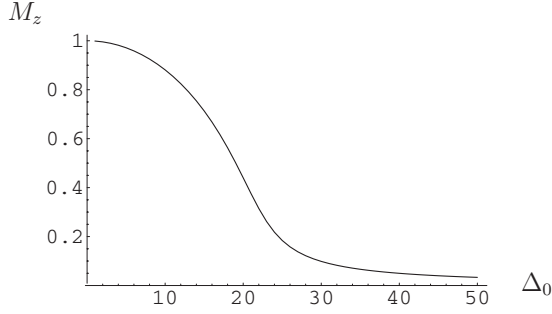
FIG. 6. The magnetization as function of transverse effective field Δ_0 is plotted for Hamiltonian (22) with $h \equiv 2A_0/7 = 1$, $V_0 = 20$. Note that for $\Delta_0 > V_0$ a remnant magnetization of magnitude h/Δ_0 is present.

at low temperatures. Below a crossover temperature $T^* = A_0^2/V_0$, one reaches a regime where $\Delta_c > V_0$, and then $\Delta_c(T)$ is given by

$$\Delta_c(T) = A_0\sqrt{(V_0/T)} \quad (T < T^*), \tag{28}$$

corresponding to a transition temperature $T_c(H_\perp) = V_0 A_0^2/\Delta_0^2$. These are the exact same formulas found above for the case $A_0 \gg V_0$. Thus, when $\Delta_0 > V_0$, the system gains more energy from fluctuations than it does from the interaction. However, since $H_\perp$ cannot flip nuclear spins, a small remnant magnetization proportional to A_0/Δ_0 allows ordering at low temperatures.

In this mean-field theory, one thus finds two regimes, The first, when $V_0 \gg A_0$ and $\Delta_0 \ll V_0$, is the standard Ising picture: At $\Delta_0 = 0$ the spins are in either state $|\uparrow\rangle$ or state $|\downarrow\rangle$, and the electronic degrees of freedom order. For finite $\Delta_0 \ll V_0$ the spins fluctuate to the excited state at energy V_0. However, when $\Delta_0 \gg V_0$ and/or in the whole parameter regime for $A_0 \gg V_0$, the physical picture is different: The relevant single Ho Ising states are the electronuclear states $|\Uparrow\rangle$, $|\Downarrow\rangle$, Eq. (A3), and the phase transition line is dictated by their $H_\perp$-dependent interaction, as discussed in Sec. IV A 1.

These two physical pictures are best illustrated by the value of the magnetization at $T = 0$. For $A_0 \gg V_0$, $M_z \propto \eta$, given in Eq. (A6). For $V_0 \gg A_0$ and $\Delta_0 \ll V_0$, expanding Eq. (B4) in Δ_0/V_0, one sees that $M_z = 1 - \Delta_0^2/(2V_0^2)$, showing that the excitation energy is V_0. However, when $\Delta_0 \gtrsim V_0$, the hy-

perfine energy dictates the magnetization, which is given by $M_z \approx A/V_0$ for $\Delta_0 = V_0$ and $M^z = A_0/\Delta_0$ for $\Delta_0 \gg V_0$ (see Fig. 6).

In Fig. 7 we plot the phase diagram of mean-field Hamiltonian (22) as a function of T and $H_\perp$ for $V_0 \gg A_0$. In the low-T regime, one can compare this with the phase diagram of a system with $A_0 \gg V_0$ and a similar value of $A_0\sqrt{V_0}$. As expected from Eq. (28), for $T \ll T^*$ the two systems have the same behavior.

In Ref. 32 a similar phase diagram was calculated for LiHoF$_4$ and compared to experiment.[1] This comparison was made by rescaling the theoretical curve to agree with the experiments at the lowest temperature. However the condition $H_\perp \ll \Omega_0/\mu_B$ is then not well satisfied at criticality, and the transverse hyperfine interactions are important. By forcing the theory and experiment to coincide in the regime where the theory is not applicable, a discrepancy with experiment over the whole temperature range is obtained [see Fig. 1b of Ref. 32]. This can be corrected for $T > 0.1$ K by choosing the scaling parameter better. However, in order to obtain a good fit with the experimental phase diagram at the lowest temperatures, one has to take into account the transverse hyperfine terms.[1] For $x < 1$ the off-diagonal dipolar interactions have to be included as well. These interactions are considered next.

B. Effect of transverse hyperfine interaction

Independent of the ratio A_0/V_0, for $\Delta_0 \gg A_0, V_0$ we found for $H_{hyp}^\perp = 0$, which is equivalent to $\Omega_0 \to \infty$, that $\Delta_c = A_0\sqrt{(V_0/T)}$, diverging as $T \to 0$. This pathology arises because we need to include the transverse hyperfine terms. With $H_{hyp}^\perp \neq 0$ the splitting $\tilde{\Delta}$ becomes appreciable for $\mu_B H_\perp \approx \tilde{\Delta}_0 \approx \Omega_0$ (in this regime $\mu_B H_\perp \approx \Delta_0$), while $V_{eff} = V_0 A_0^2/\Delta_0^2 \ll A_0$. Thus, for A_0, $V_0 \approx \Omega_0$ a quantum phase transition is obtained within the regime of the applicability of Hamiltonian (A23). The divergence of Δ_c is rounded, as we schematically draw as a solid line in Fig. 5. A similar rounding off of Δ_c occurs for $V_0 \gg A_0$ (Fig. 7).

As mentioned above, the condition $A_0 \ll \Omega_0$ is not that well satisfied in the LiHo$_x$Y$_{1-x}$F$_4$ system. Still, at low x, where $A_0 \gg V_0$, the phase transition occurs within the regime of the applicability of Hamiltonian (A23). Recall that in Fig. 4 we plot $V_{eff} \propto \langle J_z \rangle^2$ for $x = 0.167$, taking $V_{eff}(H_\perp = 0)$ to be
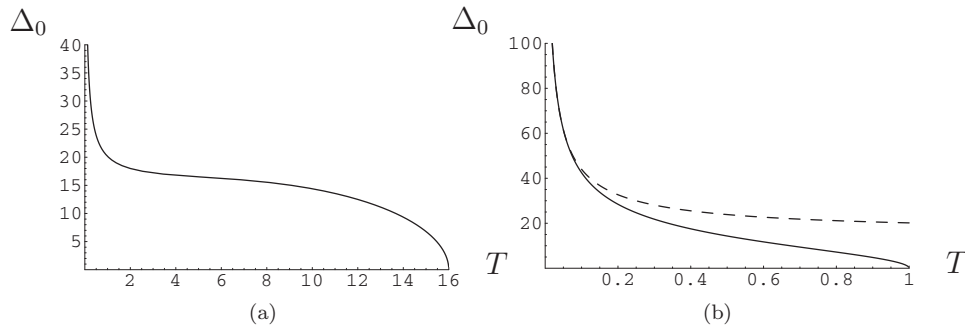

FIG. 7. (a) The phase diagram of Hamiltonian (22) for the regime $A_0 \ll V_0$, with $h \equiv 2A_0/7 = 1$, $V_0 = 16$. (b) Focusing on low temperatures, we compare the phase line in (a) (dashed line) to a system with $A_0 \gg V_0$. We take $h = 4$, $V_0 = 1$ to have the same value for $A_0\sqrt{V_0}$, so that the low-temperature divergence of the critical field is the same for the two systems.

equal to the value of $T_c=0.13$ K. The value of $H_\perp$ where $\tilde{\Delta} \approx V_{\text{eff}}$ is smaller than $H_\perp^*$. This is true for all smaller dilutions x as well. At $x=0.167$ one expects the quantum phase transition to occur at $H_\perp \approx 2$ T, where $\tilde{\Delta} \approx V_{\text{eff}}$. Thus, three energy scales govern the phase transition. The spin-spin interaction V_0 dictates T_c at zero field, the hyperfine interaction A_0 dictates the phase diagram at finite $H_\perp$, and the larger anisotropy scale Ω_0 dictates the position of the quantum critical point, since quantum fluctuations become important only when $\langle \uparrow | \mu_B H_\perp | \Gamma_2^l \rangle \approx \Omega_0$. It is for this reason[12] that in LiHo$_x$Y$_{1-x}$F$_4$ it is much easier to disorder the ordered phase thermally rather than quantum mechanically,[5] especially when $x \ll 1$.

For $x \ll 1$ one can calculate the phase diagram for LiHo$_x$Y$_{1-x}$F$_4$ including all hyperfine terms using the effective Hamiltonian derived in Sec. III. However as we have seen, at higher temperatures this Hamiltonian breaks down at quite low transverse fields, because of the mixing of higher levels (cf. Fig. 4). Therefore, for larger x, where the dipolar interactions are stronger, quantum criticality occurs at $H_\perp > H_\perp^*$, where all the nuclear levels are well mixed. This is the case for $x=1$, for which a quantum phase transition is observed at 4.9 T.[1]

We therefore adopt a different approach, which covers all values of x, and calculate the phase diagram numerically, including both $H_{\text{hyp}}^{\parallel}$ and $H_{\text{hyp}}^{\perp}$, starting from the Hamiltonian

$$H_F = \sum_j \left(H_j^{\text{cf}} - g_J \mu_B H_\perp J_j^x + A_J \vec{I}_j \cdot \vec{J}_j + \sum_i U_{ij}^{zz} J_i^z J_j^z \right),$$

(29)

in which the single spin Hamiltonian is exact. We then treat the interactions in mean-field approximation; i.e., we assume

$$\sum_i U_{ij}^{zz} J_i^z J_j^z \rightarrow U_{\text{MF}} \langle J_j^z \rangle J_j^z$$

(30)

(see also Appendix B). One of the central results of this paper is that the single atom Hamiltonian dictates much of the physics of LiHo$_x$Y$_{1-x}$F$_4$. We shall indeed see that the mean-field approximation to the interactions has only a small effect on the results.

The phase diagrams for $x=0.167$ and $x=0.045$ are drawn as dashed lines in Fig. 8. Comparing the calculation for $x=0.167$ with experiment, we see that it naturally explains why it is much harder to disorder the SG phase quantum mechanically than thermally. Going to $x=0.045$, we see that the reduction in T_c is $\propto x$, while the reduction in $H_\perp^c$ is much smaller, as can be anticipated from the requirement $V_{\text{eff}} \approx \Delta_0$ (Fig. 4).

However, the agreement with experiment is still not perfect for small x. For $x=0.167$ one obtains a larger critical field at $T=0$ and a qualitatively different behavior near $T_c(0)$. As was discussed in Ref. 12, these differences cannot be attributed to the mean-field approximation, but they testify to the inadequacy of Hamiltonian (29). This is since the behavior near $T_c(0)$ should follow Eq. (21) (for $x=0.167$ the condition $V_0 \ll A_0$ is well satisfied), and the values for Δ_c obtained at the lower temperatures in the experiment[5] necessitate the existence of appreciable quantum fluctuations
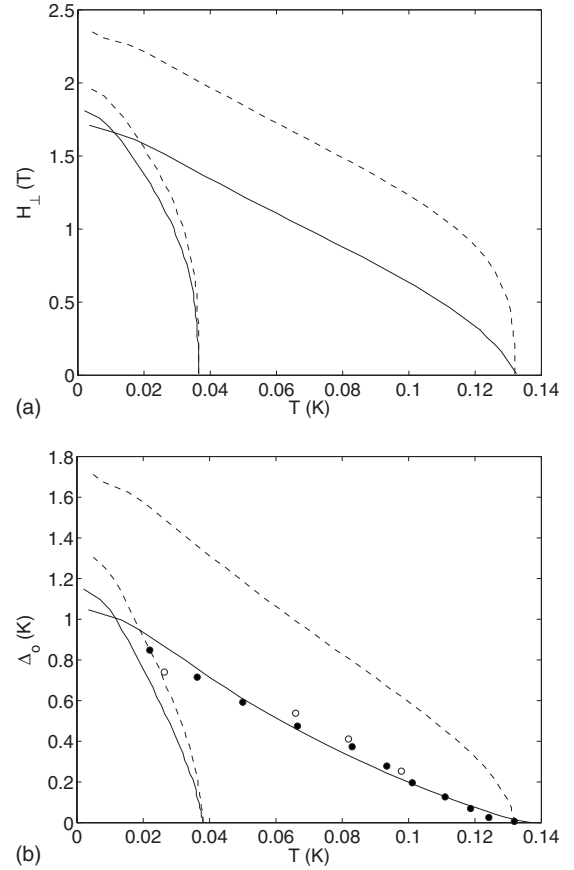

FIG. 8. (a) The phase diagrams for $x=0.167$ (thick lines) and $x=0.045$ (thin lines) as a function of $H_\perp$ and T. The solid (dashed) lines are calculated with (without) the off-diagonal dipolar interactions. The low-T, $H_\perp=0$ phase is believed to be a spin glass for both dilutions, with a crossover at finite $H_\perp$ between a quasi-spin-glass and a paramagnet. Note the "re-entrant" behavior predicted when the off-diagonal dipolar interactions are included (as seen by the crossing of the phase lines at $H_\perp \sim 1.65$ T); see text. (b) The same phase diagram as in (a) now plotted as a function of Δ_0, T, to allow comparison with experiment (Ref. 5) at $x=0.167$. Filled and empty circles, taken from Fig. 1 of Ref. 5, denote the PM-SG crossover from dynamical measurements and nonlinear susceptibility, respectively. With the inclusion of the off-diagonal dipolar interactions, good quantitative agreement is obtained.

at $H_\perp \approx 1$ T, which contradicts the results shown in Fig. 4. To explain things, we now finally turn to the nondiagonal dipolar terms.

C. Random nondiagonal dipolar terms

To account for the experimental phase diagram, one has to include the dependence of the effective field on the off-diagonal terms of the dipolar interaction.[12] These add an effective random longitudinal field and in the SG regime also enhance the effective transverse magnetic field, as explained in Appendix A 3. The random longitudinal field is crucial in dictating the nature of the phase at finite $H_\perp$, as it destroys long-range SG order.[16,19] However, at least for $x \ll 1$ it does not strongly affect the position of the phase line because: (i) the effective random longitudinal field is zero at $H_\perp=0$ and

is small for $H_\perp \ll \Omega_0/\mu_B$; (ii) it is random in sign, with only a small effect on the typical interaction; and (iii) at large $H_\perp$, where $\gamma_i^{\tilde{z}}$ is appreciable, the crossover to the PM phase depends only weakly on V_0, as can be inferred from Fig. 4.

Thus, in calculating the phase diagram, we neglect the random longitudinal fields and consider only the enhancement of the effective transverse field by the off-diagonal dipolar interactions. This enhancement depends on x and $H_\perp$; here we follow Ref. 12 in neglecting the dependence on $H_\perp$. We further assume that this enhancement is proportional to x when $x \ll 1$; i.e., we write a total transverse mean-field $\tilde{H}_\perp$ $= H_\perp + H_\perp^d$, with $H_\perp^d \propto x$. Note that this mean field is just the average of the transverse field $\tilde{H}_i^\perp$ that we discussed in Appendix A 3, i.e., $H_\perp^d = \langle \tilde{H}_i^\perp \rangle$.

This leads to satisfying quantitative agreement with the experimental phase diagram for $x=0.167$ (see Fig. 8). $T_c(0)$ $\propto V_0 \propto x$, while $H_\perp^c$ at the $T=0$ transition depends mainly on the energy scale Ω_0. For $x \leq 0.167$, $H_\perp^c$ should therefore change only slightly with dilution. The dilution dependence of $H_\perp^c$ is a result of two competing effects. First, since the transition occurs when $\tilde{\Delta} \approx V_0$, there is a slow enhancement in $H_\perp^c$ with x (slow because $\tilde{\Delta}$ varies rapidly with $H_\perp$; see Fig. 4). Second, $H_\perp^d \propto x$, giving a further reduction $\propto x$ in $H_\perp^c$. This leads to the interesting prediction that for low enough x, there will be an increase in $H_\perp^c$ with decreasing x, so that $H_\perp^c$ has a minimum at some x. This is seen in our figure by the crossing of the phase lines (see Fig. 8). In analogy with the re-entrant behavior one sees in some systems on variation of an external field, we can call this a prediction of a kind of "re-entrance" as a function of concentration x.

It is interesting that the combined effect of the hyperfine interactions and the transverse dipolar interactions leads to this re-entrant behavior. Even though the effect of the transverse dipolar interactions is only a weak effect compared to that of the hyperfine terms, it is just enough to tip the system into re-entrance. Note however that without the much stronger hyperfine effect on the phase diagram, this would not have happened. We remark again that we do not think that it is possible to explain the phase diagram without incorporating the hyperfine terms (e.g., by including only dipolar interactions;[18] cf. our discussion in Sec. III).

D. Nature of the low-temperature phase

As we have seen, it is possible to derive an accurate phase diagram without saying too much about the nature of the phases themselves. In fact the nature of the low-T phases of LiHo$_x$Y$_{1-x}$F$_4$ has been rather controversial in recent years. Here we would like to outline several rather important implications of our results. We divide our discussion between the zero transverse field case and the case of finite $H_\perp$.

1. Zero transverse field

At all dilutions, the LiHo$_x$Y$_{1-x}$F$_4$ system is PM at high temperatures. However, as mentioned above, at low temperatures the phase of the system is dilution dependent. It is well established both experimentally[2] and theoretically[33] that for $x > x_F$ the system orders ferromagnetically at low tempera-

tures, where values for x_F are in the range of 0.2–0.5. However, at low dilutions the nature of the phase is controversial. Theoretically, it is argued that a SG phase should exist at all dilutions $x \ll 1$.[34] Experimentally, it was argued that at x $=0.167$ the system has a low-temperature glass phase,[5] while for $x=0.045$ the experiment[8] revealed a very intriguing yet unexplained behavior of the imaginary part of the susceptibility, in which its width in the frequency domain *narrows* as the temperature is lowered, and it therefore received the name "anti-SG." Recently, however, these results were challenged by Jonsson *et al.*,[35] who claimed for $x=0.167, 0.045$ that there is no phase transition to the SG phase. Furthermore, their analysis suggests that the system at the above two dilutions exhibits similar characteristics. A similar controversy arose regarding the specific heat of the system and its consequences regarding the nature of the phase at $x=0.045$.[17,36] Note that it is difficult to reach equilibrium conditions both experimentally, near the transition,[35,37] and numerically, using Monte Carlo.[33] Therefore further studies will be useful in resolving the low-temperature phase of the diluted LiHo$_x$Y$_{1-x}$F$_4$.

Our analysis above does not depend on the precise nature of the ordered phase and therefore cannot lead to definite conclusions regarding this question. However, since Hamiltonian (4) gives a comprehensive description of the system down to a few millikelvins, some clarifying statements based on our analysis can be made:

(i) The only difference between the LiHo$_x$Y$_{1-x}$F$_4$ compounds at $x=0.167$ and $x=0.045$ is the strength of the dipolar interaction, both in the magnitude of the typical terms and in the distribution due to randomness. All the single Ho properties, which, as discussed above, dictate much of the physics, stay unchanged. Thus, we have every reason to believe that at $x=0.045$ the equilibrium low-temperature phase is also a spin glass. However, as shown in Fig. 8, its $T_c(0)$ is reduced to roughly 35 mK, and according to this the experiments at this dilution[8,17,35,36] were done in the PM regime.

(ii) As we show above, the dynamics of the system at low temperatures is significantly slowed down by the coupling to the nuclear spins (see also Ref. 35). Indeed, the peculiar features in the spin susceptibility at $x=0.045$ (Ref. 8) were obtained as the temperature was reduced to below 150 mK. At this temperature the higher nuclear-spin levels start to be depleted, and all but few of the Ho atoms are in either state $|\uparrow, -7/2\rangle$ or state $|\downarrow, 7/2\rangle$. Thus, the system cannot take advantage of the much faster transitions between the higher nuclear-spin states (see Fig. 4), and the dynamics slow down appreciably. The data of Quilliam *et al.*,[36] which show that the peak in the specific heat occurs in a similar temperature for $x=0.02, 0.045, 0.08$, supports the view that single spin physics and, in particular, the hyperfine interactions are significant in the interpretation of the experiments in these dilutions.

(iii) In Ref. 17 it was argued that for $x=0.045$ the internal transverse field resulting from the off-diagonal terms of the dipolar interaction stabilize a low-temperature spin liquid state. It was further argued there that this is correct also for transverse fields which are effectively reduced by a factor of 10^4. The analysis in Ref. 17 was done in the electronic degrees of freedom. However, in the regime relevant to the

experiment,[8] effective Hamiltonian (A23) is valid, with zero random longitudinal field. Therefore, the analysis should be done considering the electronuclear degrees of freedom, within the framework of Hamiltonian (A23). In particular, the effective transverse field due to the off-diagonal dipolar interactions at $H_\perp = 0$ is much smaller than the values considered in Ref. 17, as can be inferred from the logarithmic scale graph in Fig. 4.

2. Finite transverse field

Turning now to nonzero $H_\perp$, we note first that there is a crucial difference between the FM phase and the SG phase if the latter exists at $H_\perp = 0$. In the FM regime the lower critical dimension $d_c = 2$ (cf. Ref. 38), and in three dimensions the FM phase is stable to a small random field. Thus we expect that the FM phase, which exists for large x, will survive at finite $H_\perp$.

However, if one supposes that for intermediate x one has a SG phase at $H_\perp = 0$, then the critical dimension is $d_c = \infty$ (cf. Refs. 39 and 40), and so the long-range SG order should be destroyed by an infinitesimal random field.[16,19] As is well known, this means that the system will no longer be a homogeneous SG, but instead domains of finite size will be created: Each one will have internal SG order but the order will be uncorrelated between different domains. The correlation length ξ, which is essentially the domain size, is given by[16,19]

$$\xi \approx \left(\frac{\Omega_0}{\mu_B H_\perp} \right)^{1/[(3/2)-\theta_d]}. \tag{31}$$

where $\theta_d \approx 0.2$ is the stiffness exponent.[39,40] Essentially the system is able to gain energy from the random field by creating domains. Referring to Eq. (A27), we see that this energy gain is a result of the two terms in the numerator contributing with the same sign, i.e., an effective enhancement of the transverse magnetic field.

V. EXPERIMENTAL CONSEQUENCES

In this paper we have derived results regarding the single-particle properties of the Ho ion in the LiHo$_x$Y$_{1-x}$F$_4$ systems, as well as the phase diagram. We have also addressed the regime where $A_0 \ll V_0$, which is not applicable to the LiHo$_x$Y$_{1-x}$F$_4$ system but is the more abundant regime in general. In this section we address the relation between our results and possible experiments.

A. Single spin properties

A central result of this paper is the derivation of the low-energy effective Hamiltonian for the LiHo$_x$Y$_{1-x}$F$_4$ system as a generalized Ising Hamiltonian in the electronuclear degrees of freedom [Eq. (18)]. This effective Hamiltonian is completely determined by the effective random fields γ_i^z and the single-ion parameters ϵ_m, $\widetilde{\Delta}_m$, and η_m [see Eq. (A16)], the last one determining the effective spin and therefore the effective spin-spin interaction. Below we suggest magnetic-resonance and muon-spin-relaxation (μSR) experiments that
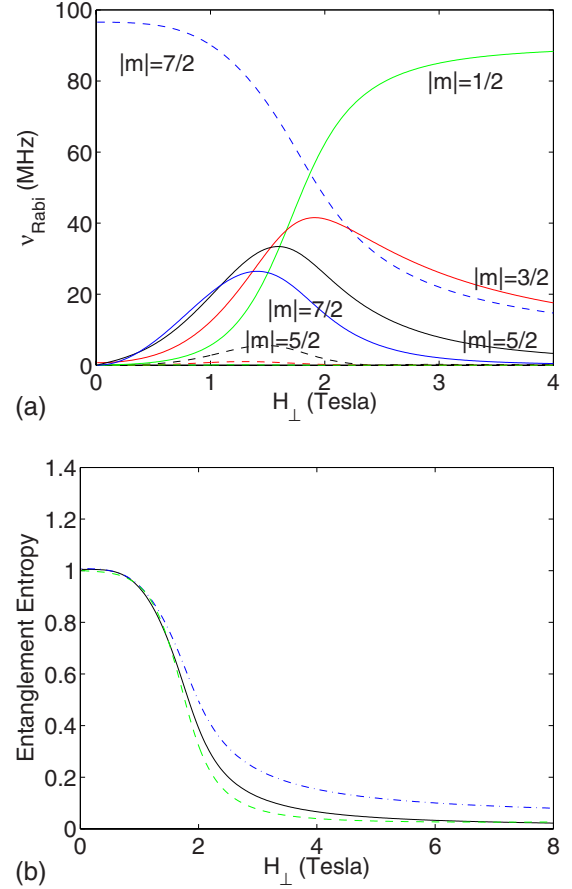

FIG. 9. (Color online) (a) Rabi frequencies of magnetic-resonance transitions to electronuclear levels within the space of the electronic Ising doublet for oscillating field along $\hat{z}$ with amplitude of 1mT as a function of a transverse magnetic field. All transitions are to antisymmetric states (dashed blue levels in Fig. 3). The dashed (solid) lines correspond to levels within the lower (upper) 8 states. (b) Entanglement entropy of the ground state as a function of $H_\perp$ (solid black line). Plotted for comparison are the normalized Rabi frequency to level 2 (first excited state; blue dot-dashed line) and the subtraction from unity of the normalized Rabi frequency to level 9 (green dashed line).

can measure the single-ion parameters directly and verify the mechanism leading to the enhancement of the effective transverse field and the emergence of an effective random longitudinal field. With regard to magnetic-resonance experiments, we give explicit quantitative predictions for the Rabi frequency of excitations to various levels. We interpret these predictions in terms of the calculated entanglement entropy of the ground state as a function of transverse field, in agreement with our analysis in Sec. II C.

1. Magnetic-resonance experiments

One obvious way of probing the low-energy properties of the LiHo$_x$Y$_{1-x}$F$_4$ system is via magnetic-resonance experiments. Specifically, such experiments can be used to quantify ϵ_m, $\widetilde{\Delta}_m$, and the nature of the wave functions as a function of $H_\perp$. In Fig. 9(a) we plot the Rabi frequencies, given by

$$\nu_{\text{Rabi}} = \frac{2b_z |\langle 1|g_J \mu_B J_z + g_N \mu_N I_z|2\rangle|}{h}, \tag{32}$$

for a magnetic-resonance transition between the ground state and excited states as a function of transverse field H_x for an ac field along $\hat{z}$. Only the lowest 16 levels are considered. From symmetry, only transitions to antisymmetric states (plotted dashed line in Fig. 3; see also the discussion in Sec. II C) are possible. For $H_\perp \to 0$ the only allowed transition is to the first excited state, in agreement with the form of the electronuclear states in Eq. (A3), in terms of which effective Hamiltonian (3) is written. A finite Rabi frequency to other states is allowed at $H_x \neq 0$, a consequence of the mixing of the states in Eq. (A3) resulting from $H_{\text{hyp}}^\perp$, and is thus larger for larger $|m|$. As discussed in Sec. II C, with increasing H_x the electronic and nuclear spins disentangle, and the electronic state at high fields is approximately the symmetric state $(|\uparrow\rangle + |\downarrow\rangle)/\sqrt{2}$ for the lower eight states and the antisymmetric state $(|\uparrow\rangle - |\downarrow\rangle)/\sqrt{2}$ for the upper eight states. For this reason, except for the first excited state at small H_x, the Rabi frequency is larger to the states in the upper group. At large H_x the Rabi frequency to state 9 (the lowest level in the upper group) dominates, in agreement with the picture (see Sec. II C) that levels in the lower and upper groups of eights have similar nuclear states, respectively.

The disentanglement of the electronic and nuclear states can be quantified by calculating, as a function of H_x, the entanglement entropy $-\text{Tr}(\rho_I \log \rho_I)$, where

$$\rho_I \equiv \sum_M \langle M|\text{g.s.}\rangle\langle\text{g.s.}|M\rangle \tag{33}$$

is the reduced density matrix in the subsystem of the nuclear spin. The entanglement entropy is shown for the ground state as a solid line in Fig. 9(b). We replot as a dashed line the Rabi frequency to the first excited state scaled to 1 at $H_x = 0$. We plot $1 - \tilde{\nu}_{\text{Rabi}}(9)$ as a dotted dashed line, where $\tilde{\nu}_{\text{Rabi}}(9)$ is the scaled Rabi frequency to level 9. Although not exact, we see that the diminishing of $\nu_{\text{Rabi}}(2)$ and the emergence of $\nu_{\text{Rabi}}(9)$ with increasing field is a measure of the (dis)entanglement of the electronic and nuclear spins. A naive conclusion from the above would be that for large $H_\perp$ the nuclear spins decouple from the electronic spins and therefore effective Hamiltonian (1) is recovered. The fact that for $x = 1$ the soft mode is gapped near the quantum phase transition (at 4.9 T) (Refs. 14 and 15) suggests that this simplified model is not suitable also in this regime.

In Fig. 10 we plot the Rabi frequency as a function of H_x for an ac field in the x direction. The relevant matrix element is then $\langle 1|g_J \mu_B J_x + g_N \mu_N I_x|2\rangle$. The operator J_x changes the z component of the electronic spin. The relevant matrix element is then proportional to the amplitude of $|\Gamma_2^l\rangle$ in the ground state. This amplitude, resulting from the transverse hyperfine interaction, is small, $\sim O(A_0/\Omega_0) \approx 10^{-2}$, and at $H_x = 0$ is finite only for the state with $|I_z| = 5/2$. This is why the intensity for a longitudinal ac field is so much larger than that for a transverse ac field [compare Figs. 9(a) and 10]. For an ac field along $\hat{z}$, only transitions to symmetric states (plotted as solid curves in Fig. 3) are possible.
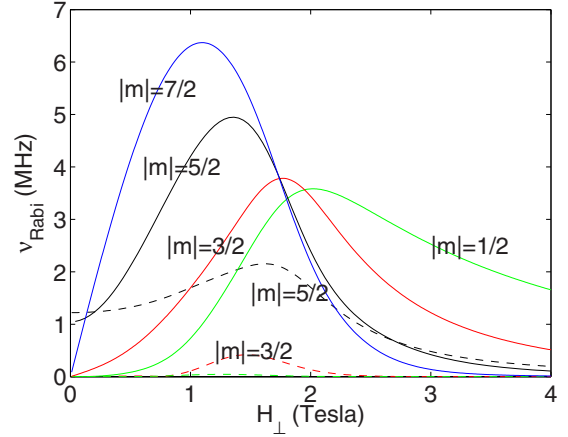

FIG. 10. (Color online) Rabi frequency of magnetic-resonance transitions for an ac field in the x direction. Details are as in Fig. 9 except that here the transitions are to symmetric states (solid green levels in Fig. 3).

From the picture of the system without the transverse hyperfine interaction, where the 16 states at zero field are eigenstates of I_z, one might expect that for a transverse ac field the dominant intensity would come from the nuclear operator. Surprisingly, it is the electronic operator that dominates the magnetic-resonance experiment. This is because $A_0/\Omega_0 \gg \mu_N/\mu_B$. Thus, although the levels are predominantly nuclear-spin levels, the relevant experiment is basically an electron-spin-resonance (ESR) experiment.

All the results above are valid for single Ho ions and can be checked in very dilute samples, where interactions are negligible. For larger x, in the SG regime, the interplay between the off-diagonal dipolar interactions and the applied transverse field results in an effective enhancement of the transverse field and the emergence of an effective random field[12,16] (see details in Appendix A 3). This result, shown in Secs. IV C and IV D 2 to be crucial for the structure of the phase diagram in the SG regime[12] as well as for the nature of the phase itself,[16,19] can actually be verified by measuring, e.g., $\nu_{\text{Rabi}}(2)$ as a function of $H_\perp$ for different x. The off-diagonal dipolar interactions should lead not only to a dispersion in $\tilde{\Delta}_{7/2}$ but also to an x-dependent shift upward of its mean value. This shift can be checked against our approximation in Sec. IV C.

2. μSR experiments

According to Eq. (A6), the single Ho spin moment at low temperatures $\propto \eta$, and so it decreases with $H_\perp$. Such a field dependence of the individual magnetic moments could be directly measured using μSR. The magnetic field at the muon site is proportional to the magnetic moment size of the material, which in a diluted sample is given by the nearest Ho ion. Such a measurement should be done at dilution $x \ll 1$, both because our prediction is for the regime where $A_0 > V_0$ and because then the contribution from more distant Ho ions will be smaller.

B. LiHo$_x$Y$_{1-x}$F$_4$ phase diagram

In Sec. IV C we have given explicit quantitative predictions for the phase diagram of the LiHo$_x$Y$_{1-x}$F$_4$ system as a

function of x. Our results for $x=0.0167$ are in good agreement with experiment, and our predictions regarding the phase diagram at $x=0.045$, as well as the re-entrant crossover field as function of dilution, can be checked experimentally in a straightforward way. However, here we would like to suggest an experiment that would directly probe the significance of the hyperfine interactions in dictating the phase diagram of the LiHo$_x$Y$_{1-x}$F$_4$ system at low x.

We use the above result, predicting that at $H_x \approx 2-3$ T, the magnetic-resonance intensities for transitions to levels with $|I_z|=1/2$, $3/2$ are appreciable. Thus, one could in principle, by populating these states, change the critical field at low T: A nonequilibrium occupation of these excited electronuclear levels would lead to stronger quantum fluctuations (cf. Fig. 4) and therefore to a lower critical field. This opens up the rather fascinating possibility of controlling the quasi-equilibrium phase diagram of the system by driving a steady-state nonequilibrium nuclear-spin population.

C. Limitations of the LiHo$_x$Y$_{1-x}$F$_4$ system

The LiHo$_x$Y$_{1-x}$F$_4$ compound is a particularly useful test system: It is a well-defined Ising system, with a doubly degenerate ground state. Quantum fluctuations are easily tunable at moderate transverse fields, and x can be varied over a huge range. However, there are at least two limitations on this system, viz.:

(i) The allowed values of the dipolar spin-spin interaction V_0, hyperfine interaction A_0, and crystal anisotropy energy Ω_0 do not test the whole parameter range. Thus, e.g., to observe our prediction that the hyperfine coupling dictates a diverging H_c at low T for either $A_0 \ll V_0$ or $A_0 \gg V_0$ given that A_0, $V_0 \ll \Omega_0$ (see Figs. 5 and 7), we need a system where the latter condition is well satisfied.

(ii) For $H_\perp = 0$, the ground state is degenerate. Inducing quantum fluctuations coupling the two ground states requires a transverse field. However, the application of $H_\perp$ results in an emerging random field. As a result, the quantum phase transition between the SG and FM phases cannot be seen as a function of $H_\perp$ but only as a function of a parameter that does not break time-reversal symmetry, e.g., pressure.[16] To observe such a transition one would need a system where quantum fluctuations between the Ising ground states are appreciable at $H_\perp = 0$. One would then have to tune the dilution so that at ambient pressure the typical spin-spin interactions are of the order of the quantum fluctuations and to look for the transition as a function of pressure.

VI. CONCLUSIONS

In this paper we have considered anisotropic quantum magnetic systems in which both dipolar and hyperfine interactions play a role. We have shown that the transverse field Ising model is not sufficient to describe such systems. Instead, we have given a theoretical treatment of an electronuclear quantum Ising model which can do the job. The hyperfine interactions set the scale for the field at the quantum critical point, even in systems in which the hyperfine interaction is weaker than the dipolar spin-spin interaction. We

have given a detailed treatment of the LiHo$_x$Y$_{1-x}$F$_4$ compound, calculating the phase diagram for all dilutions x and giving explicit numerical results for $x=0.045$ and $x=0.167$. We explain the experimental result that thermal fluctuations more easily destabilize the ordered phase than quantum mechanical fluctuations do. Off-diagonal dipolar interaction terms are shown to reduce the transverse critical field $H_c^\perp$, and a prediction for a nonmonotonic critical field as a function of x is given. The experimental consequences of our results as well as possible measurements of the parameters of the effective Hamiltonian are discussed.

We note that our results have wider implications in two ways, which will be explored elsewhere. First, as just noted, they can be applied to many other dipolar quantum magnets. Second, the nuclear spins will clearly have an even more profound effect on the dynamical properties of these systems than on the phase diagram. Indeed, the big surprise is quite how important they are for the thermodynamics, even when $A_0 \ll V_0$.

Our prediction for the re-entrance of the crossover field as a function of dilution was coincidentally and independently discovered experimentally by Ancona-Torres *et al.*[41]

ACKNOWLEDGMENTS

APPENDIX A: DERIVATION OF THE EFFECTIVE HAMILTONIAN

In this appendix we derive the effective Hamiltonian in Eq. (18).

1. Ising-type terms

We are interested in the $2I+1$ lowest levels, shown for the 16 levels of the Ho ion in LiHo$_x$Y$_{1-x}$F$_4$ in Fig. 2. The term $H_1^\perp$ in Eq. (15) has zero matrix element between any of these 16 low-energy states and thus must mix higher crystal-field states. This results in contributions of order V_0/Ω_0, $A_J/\Omega_0 \ll 1$. We therefore begin by discussing in this subsection the longitudinal interaction terms, i.e., the Hamiltonian $H_l = H_0 + H_1^{zz}$.

In the subspace of the lowest $2I+1$ electronuclear states, we have seen that H_l reduces to

$$H_{el} = \sum_i \omega_0 \tau_i^z I_i^z - \sum_{i,j} V_{ij}^{zz} \tau_i^z \tau_j^z - \sum_i \Delta_0 \tau_i^x. \quad \text{(A1)}$$

Let us first discuss this Hamiltonian for $T \ll \omega_0$. Then, one can simplify the model to include only the levels with $I_z = \pm I$ (i.e., with $I_z = \pm 7/2$ for LiHo$_x$Y$_{1-x}$F$_4$), described in Sec. II B. The effective Hamiltonian then reduces to[12]

$$H_{le} = 2A_0 \sum_i \tau_i^z \sigma_i^z - \sum_{i,j} V_{ij}^{zz} \tau_i^z \tau_j^z - \sum_i \Delta_0 \tau_i^x, \quad \text{(A2)}$$

where τ_i acts upon the two electronic states $|\uparrow\rangle$, $|\downarrow\rangle$ at site i, σ_i acts upon the two nuclear-spin states with $I_z = \pm 7/2$, and the coupling $A_0 = I\omega_0 \sim 0.7$ K.

For $H_\perp \neq 0$ the two low-energy Ising doublet states are given by[12]

$$| \Uparrow \rangle = c_1 |a\rangle + c_2 |b\rangle,$$

$$| \Downarrow \rangle = c_1 |\bar{a}\rangle + c_2 |\bar{b}\rangle, \quad (A3)$$

where $|a\rangle$, $|b\rangle$, $|\bar{a}\rangle$, and $|\bar{b}\rangle$ are defined in Sec. II B and

$$c_1 = \alpha \Delta_0, \quad c_2 = \alpha[A_0 - \sqrt{A_0^2 + \Delta_0^2}], \quad (A4)$$

$$\alpha = [\Delta_0^2 + (A_0 - \sqrt{A_0^2 + \Delta_0^2})^2]^{-1/2}. \quad (A5)$$

Thus, as noted just above, the longitudinal part of the hyperfine interaction blocks quantum fluctuations between the relevant Ising states.

It then follows that a transverse field $H_\perp \ll \Omega_0$ can only renormalize the effective spin of what is just a *classical* Ising system: One finds

$$\langle \tau_\pm^z (H_\perp) \rangle = \eta \langle \tau_\pm^z (0) \rangle, \quad \eta = (c_1^2 - c_2^2), \quad (A6)$$

with $\langle \tau_-^z \rangle = -\langle \tau_+^z \rangle$. Note that

$$\eta = 1 - \frac{\Delta_0^2}{2A_0^2} \quad (\Delta_0 \ll A_0),$$

$$\eta = A_0/\Delta_0 \quad (\Delta_0/A_0 \gg 1). \quad (A7)$$

Absorbing this renormalization into the dipolar interaction, H_{le} [Eq. (A2)] reduces to

$$H_{\rm eff}^\parallel = -\sum_{i,j} \widetilde{V}_{ij}^{zz} s_i^z s_j^z \quad (H_\perp \ll \Omega_0/\mu_B), \quad (A8)$$

$$\widetilde{V}_{ij}^{zz} = \eta^2 V_{ij}^{zz}, \quad (A9)$$

where $\hat{s}_j$ is a spin-half matrix operating on the states $|\Uparrow\rangle$ and $|\Downarrow\rangle$ of the jth spin, such that $\hat{s}_j^z |\Uparrow\rangle = |\Uparrow\rangle$, $\hat{s}_j^z |\Downarrow\rangle = -|\Downarrow\rangle$, etc.

Thus we have shown the equivalence of the two Hamiltonians H_{le} in Eq. (A2) and $H_{\rm eff}^\parallel$ in Eq. (A9). Both are applicable in the low-T limit $kT \ll \omega_0$ when $H_\perp \ll \Omega_0$.

For higher temperatures, $\omega_0 \lesssim T \ll \Omega_0$, Hamiltonian (A1) has to be considered. Following the arguments above, only levels with the same I_z mix (see Fig. 2). The generalization of Eqs. (A3)–(A5) results in

$$|\Uparrow, m\rangle = c_{1m} |\uparrow, m\rangle + c_{2m} |\downarrow, m\rangle,$$

$$|\Downarrow, -m\rangle = c_{1m} |\downarrow, -m\rangle + c_{2m} |\uparrow, -m\rangle, \quad (A10)$$

with coefficients

$$c_{1m} = \alpha_m \Delta_0,$$

$$c_{2m} = \alpha_m [m\omega_0 + \sqrt{m^2 \omega_0^2 + \Delta_0^2}], \quad (A11)$$

and

$$\alpha_m = [\Delta_0^2 + (m\omega_0 + \sqrt{m^2 \omega_0^2 + \Delta_0^2})^2]^{-1/2}. \quad (A12)$$

If we choose $m = -I$, these equations revert to Eqs. (A3)–(A5) for the two lowest levels.

We now define a set of pseudospin $-1/2$ degrees of freedom $\{\hat{s}_{im}\}$, operating in the subspace spanned by the pair of degenerate levels $|\Uparrow, m\rangle$, $|\Downarrow, -m\rangle$. In terms of these pseudospins, we then obtain for the Hamiltonian H_l defined above [Eq. (A1)] the renormalized effective Hamiltonian

$$H_{\rm eff}^\parallel = \sum_{jm} n_{jm} \epsilon_m(H_\perp) - \sum_{i,j;m,m'} n_{im} n_{jm'} \widetilde{V}_{im,jm'}^{zz}(H_\perp) s_{im}^z s_{jm'}^z, \quad (A13)$$

where we have defined a pseudospin occupation number n_{jm} such that $\sum_m n_{jm} = 1$ and we have defined energies

$$\epsilon_m(H_\perp) = {\rm sgn}(m) \sqrt{(m^2 \omega_0^2 + \Delta_0^2)}, \quad (A14)$$

$$\widetilde{V}_{im,jm'}^{zz} = \eta_m \eta_{m'} V_{ij}^{zz} \quad (A15)$$

and a renormalization factor

$$\eta_m = (c_{1m}^2 - c_{2m}^2). \quad (A16)$$

Thus again we obtain a generalized classical Ising model, now involving the entire set $\{\hat{s}_{im}\}$ of pseudospins. There are $2I+1$ pseudospins per site (only one of which is occupied at any time), interacting with pseudospins at the other sites.

We emphasize that Hamiltonians (A1) and (A13) are entirely equivalent. The great advantage of Eq. (A13) [and its low-T simplification in Eq. (A9)] is that the physics is correctly displayed, that of a classical Ising system. This is done using the physically meaningful energy scales for this regime.

2. Transverse hyperfine terms

Now suppose we neglect all dipolar interactions between the electronic spins, but we now switch on the full hyperfine coupling, including the transverse hyperfine term. The general effect of this is seen in a plot (Fig. 3) of the 16 relevant eigenenergies for the Ho ion in the LiHo$_x$Y$_{1-x}$F$_4$ system as a function of $H_\perp$.

As $H_\perp$ increases, levels separate into two groups of eights, given by symmetric and antisymmetric combinations of states with the same m. Each pair of levels $|\Uparrow, m\rangle$, $|\Downarrow, -m\rangle$ which is related by time-reversal symmetry is then split by the combination of $H_\perp$ and $H_{\rm hyp}^\perp$.

If we wish to write an effective Hamiltonian for this system in the original basis of $2I+1$ levels, we get a rather interesting result. After truncating the full $H_{\rm cf}$ down to the two lowest electronic levels, we can write for a *single ion* (ignoring now all interactions between ions) the following:

$$H_i^{\rm eff} = -\frac{1}{2} \sum_j \Delta_0 [\tau_j^+ e^{i\hat{\mathbf{A}}[\mathbf{I}_j]} + {\rm H.c.}] + \omega_0 \sum_i \tau_i^z \hat{I}_i^z, \quad (A17)$$

where the matrix element $U_j^{\rm fi} = \langle f| e^{i\hat{\mathbf{A}}[\mathbf{I}_j]} |i\rangle$ is defined between an initial state $|i\rangle = |\uparrow j; \chi_i(\mathbf{I}_j)\rangle$ before the electronic spin flips and a final state $|f\rangle = |\downarrow j; \chi_f(\mathbf{I}_j)\rangle$ after it flips, involving some initial and final nuclear-spin wave functions $\chi_i(\mathbf{I}_j)$ and $\chi_f(\mathbf{I}_j)$. The operator $\hat{U}^{(j)}$ is defined as

$$\hat{U}_j = e^{i\hat{\mathbf{A}}[\mathbf{I}_j]} \equiv \exp\frac{i}{\hbar}\int_{\Uparrow}^{\Downarrow} dt H_{\text{hyp}}^{\perp}(\mathbf{I}_j, t). \qquad \text{(A18)}$$

In general the $(2I+1) \times (2I+1)$ matrix $\hat{\mathbf{A}}[\mathbf{I}]$, which operates in the Hilbert space of $\mathbf{I}_j$, causes transitions between different hyperfine levels when the central spin (here the Ho spin) flips. A calculation of $\hat{\mathbf{A}}[\mathbf{I}]$ is actually quite lengthy, since typically it involves multiple transitions between the nuclear-spin states. Thus Hamiltonian (A17) is in general a rather complicated object, taking the form of a $(2I+1) \times (2I+1)$ matrix acting on the lowest states of the system. For LiHo$_x$Y$_{1-x}$F$_4$ this means a 16×16 matrix, which is quite unwieldy.

In the present paper we are interested only in the thermodynamic properties of our system. This allows a considerable simplification, which we can see most simply by rewriting Hamiltonian (A17) for an isolated ion (i.e., again ignoring dipolar interactions) in terms of our pseudospins, in the following form:

$$H_i^{\text{eff}} = \sum_m H_m^o(\hat{s}_{im}) + \sum_{m \neq m'} \delta\tilde{H}_{mm'}(\hat{s}_{im}, \hat{s}_{im'}), \qquad \text{(A19)}$$

where the "diagonal" terms have the matrix form

$$H_m^o = \begin{pmatrix} \epsilon_m & \tilde{\Delta}_m \\ \tilde{\Delta}_m^{\dagger} & \epsilon_m \end{pmatrix} \qquad \text{(A20)}$$

in the basis where $\hat{s}_{im}^z$ is diagonal and the nondiagonal terms couple different pseudospins.

We look first at the diagonal terms. The diagonal energies ϵ_m [Eq. (A14)] are just the eigenvalues of H_0 in Eq. (15). In zero field one has from Eq. (13) that $\epsilon_m \sim m\omega_0$ for LiHo$_x$Y$_{1-x}$F$_4$, with splitting of ~ 205 mK between adjacent pairs of levels in the Ho ion. At low $H_\perp$ the transition terms $\tilde{\Delta}_m$ split each pair of degenerate m states into the symmetric and antisymmetric combinations $|\pm, m\rangle = (|\Uparrow, m\rangle \pm |\Downarrow, -m\rangle)/\sqrt{2}$. The $\tilde{\Delta}_m$ are just the quantum fluctuation amplitudes between the eigenstates $|\Uparrow, m\rangle$ and $|\Downarrow, -m\rangle$ of the classical Ising system, induced by the transverse hyperfine coupling.

Now consider the nondiagonal term $\delta\tilde{H}_{mm'}(\hat{s}_{im}, \hat{s}_{im'})$ in Eq. (A19). The crucial point here is that when $H_\perp/\Omega_0 \ll 1$, this term will be unimportant for the phase diagram because a nondiagonal coupling between different pseudospins $\hat{s}_{im}$, $\hat{s}_{im'}$ involves a sequence of $|m-m'|$ nuclear flips. If we call these nondiagonal matrix elements $\tilde{\Delta}_{mm'}$, then for $H_\perp/\Omega_0 \ll 1$ $\tilde{\Delta}_{mm'} \ll \omega_0$ and so it can hardly affect the level spacing or any other thermodynamic properties. Thus, as far as the thermodynamics is concerned, we can get away with using the form H_m^o in Eq. (A20) when $H_\perp/\Omega_0 \ll 1$.

Summarizing, including the transverse hyperfine terms, the effective low-energy Hamiltonian for a single ion can be written as

$$H_i^{\text{eff}} \sim \sum_{i,m} n_{im}[\epsilon_m(H_\perp) - \tilde{\Delta}_m(H_\perp) s_{im}^x], \qquad \text{(A21)}$$

where both ϵ_m and $\tilde{\Delta}_m$ depend on the transverse field. If we now include back the longitudinal dipolar interaction, we obtain the Hamiltonian

$$H_{\text{eff}} = -\sum_{i,j,m,m'} \tilde{V}_{im,jm'}^{zz}(H_\perp, \omega_0) n_{im} n_{jm'} s_{im}^z s_{jm'}^z$$
$$-\sum_{i,m} n_{im}[\epsilon_m + \tilde{\Delta}_m(H_\perp, \omega_0) s_{im}^x], \qquad \text{(A22)}$$

which is the generalization of Eq. (A13) that now includes quantum fluctuations.

At very low temperatures, $T \ll \omega_0$ (which for $x \ll 1$ include the whole phase diagram), only the two lowest electronuclear states are relevant. The above Hamiltonian reduces to[12]

$$H = -\sum_{i,j} \tilde{V}_{ij}^{zz}(H_\perp) s_i^z s_j^z - \tilde{\Delta}(H_\perp) \sum_i s_i^x, \qquad \text{(A23)}$$

which is just Eq. (A9) with the addition of quantum fluctuations and is the ENQI Hamiltonian given in Eq. (2).

We are still not quite finished. We must finally add in transverse dipolar terms, which introduce one further modification to the effective Hamiltonian.

3. Nondiagonal dipolar interactions

The "nondiagonal" dipolar terms $U_{ij}^{\perp}$ couple the Ho spins in higher order in the small parameter $U_{ij}^{\perp}/\Omega_0$, and so they have typically been neglected when discussing anisotropic dipolar systems, including LiHoF$_4$. However, in Refs. 12, 16, and 19 it was shown that terms $\sim J_j^z J_i^x$ can be rather important. For $x=1$ these terms cancel by symmetry but not for $0 < x < 1$, where even when $H_\perp = 0$ they induce quantum fluctuations.[17] For $H_\perp \neq 0$ these terms can enhance or reduce the quantum fluctuations induced by the applied field. To quantify this effect, let us consider the regime $H_\perp \ll \Omega_0$ and write the original Hamiltonian in Eq. (4) or Eq. (14) as

$$H = H_{\text{long}} + H_{\text{trans}}, \qquad \text{(A24)}$$

where

$$H_{\text{long}} = H_{\text{cf}} + H_{\text{hyp}}^{zz} + U_{\text{dip}}^{zz} \qquad \text{(A25)}$$

and

$$H_{\text{trans}} = -\sum_i g_J \mu_B H_\perp J^x + \sum_{ij} U_{ij}^{zx} J^z J^x. \qquad \text{(A26)}$$

Here we neglect $H_{\text{hyp}}^{\perp}$ and all terms other than U_{ij}^{zx} in $U_{\text{dip}}^{\perp}$ which do not contribute in lowest order of perturbation theory.[16,19]

H_{long} has a low-T ordered phase, which, depending on the dilution, is FM or a SG.[2,3,33] Let us denote either of the two symmetry broken ground states of the ordered phase by ψ_0. Introducing H_{trans} as a perturbation lowers the energy of ψ_0 by[16,19,20]

$$E_\psi^{(2)} = -\frac{\langle\psi_o|\left(\sum_{i\neq j} U_{ij}^{zx} J_i^z J_j^x + g_J\mu_B H_\perp \sum_i J_i^x\right)^2|\psi_o\rangle}{\Omega_0}.$$

(A27)

Thus, the off-diagonal dipolar terms add to the applied transverse field a term,

$$H_x^{(r)}(\mathbf{r}_i) = \frac{\sum_j U_{ij}^{zx}\langle J_i^z\rangle}{g_J\mu_B}.$$

(A28)

This additional field is random in sign and can enhance or decrease the quantum fluctuations generated by the applied field $H_\perp$. Since enhancing quantum fluctuations reduces the energy of the system, configurations in which $H_x^{(r)}$ is in the direction of the applied field are energetically favorable. The terms in Eq. (A27) proportional to $H_\perp^2$ and to U^2 are independent of the spin configuration of the system. However, the cross term depends on the location and orientation of the spins and results in an effective random longitudinal field[16,19,20] $\gamma_i^z(H_\perp)$ given by

$$\gamma_i^z = \frac{2\mu_B H_\perp J^2}{\Omega_0}\sum_j U_{ji}^{zx} = c_i\frac{2\mu_B H_\perp J^2}{\Omega_0}U_0,$$

(A29)

where $J=\langle J_z\rangle\approx 5$ is the single spin magnetic moment, c_i is a random number with $\langle c_i\rangle=0$, and $\mathrm{Var}(c_i)\equiv c^2(x)$ is dilution dependent. For $(1-x)\ll 1$ we have $c(x)=c'(1-x)$,[20] with $c' \approx 1$. Note that the effective random field exists both in the SG (Refs. 16 and 19) and in the FM (Ref. 20) regimes. The randomness is a result of the quenched disorder, so the interplay between the applied transverse field and the off-diagonal dipolar terms converts spatial disorder to randomness in the effective longitudinal field. Unlike the quantum fluctuation amplitudes $\widetilde{\Delta}_m$, this random field is independent of m to zeroth order in ω_0/Ω_0.

It is clear from the definitions of the additional transverse field $H_x^{(r)}(\mathbf{r}_i)$ that its actual values and distribution depend on the particular configuration adopted by the $\{s_{im}^z\}$ in the phase of interest. Thus this final term in the effective Hamiltonian actually depends on what state the system is in. In general this extra field simply renormalizes the total field acting on the system; we have a new transverse field

$$\widetilde{H}_i^\perp = H_\perp + H_x^{(r)}(\mathbf{r}_i).$$

(A30)

This means that all the parameters in the effective Hamiltonian that formally depend on the transverse field must now depend on $\widetilde{H}_i^\perp$ rather than $H_\perp$. This inevitably introduces some randomness in these parameters, from one site to another. However, as discussed in Sec. IV D, in the SG regime, the system forms finite-size domains that maximize the energy gain from the random field γ_i^z. This is actually done by having a finite average value for $H_x^{(r)}(\mathbf{r}_i)$ in the direction of $H_\perp$, thus increasing quantum fluctuations, and this results in an effective enhancement of the applied magnetic field. With the addition of the effective random field and the effective enhancement of the transverse field, we obtain the effective Hamiltonian in Eq. (18).

APPENDIX B: CLASSICAL ISING LIMIT IN MEAN FIELD

In this appendix we derive Eq. (26). Consider a given site i with local longitudinal field H_i. We assume that as we cross the transition line into the SG phase, the expectation value of each spin grows at the same rate, i.e., $\langle\tau_j^z\rangle=\alpha_{ij}\langle\tau_i^z\rangle$. It then follows that

$$H_i = V_i\langle\tau_i^z\rangle,$$

(B1)

with $V_i=\sum_j V_{ij}^{zz}\alpha_{ij}$. Now the partition function becomes $Z=\Pi_i Z_i$, with

$$Z_i = \mathrm{Tr}(\exp\{-\beta[(hI_i^z - H_i^z)\tau_i^z - \Delta_0\tau_i^x]\}),$$

(B2)

and the average magnetization of spin i is given by

$$\langle\tau_i^z\rangle = \frac{1}{Z_i}\mathrm{Tr}(\tau_i^z\exp\{-\beta[(hI_i^z - H_i^z)\tau_i^z - \Delta_0\tau_i^x]\}).$$

(B3)

Equations (B2) and (B3) are generalizations of Eqs. (6) and (10) of Ref. 32 to the case where V_i is site dependent. Note that V_i is positive by definition. Assume now that the PM–SG phase transition occurs when the mean-field equation gives a finite magnetization for spins at sites with some typical $V_i=V_0$. Then, defining $M_z\equiv\langle\tau^z\rangle$, one obtains

$$M_z = \frac{\sum_m \frac{hm + V_0 M_z}{\bar{H}(m)}\sinh[\beta\bar{H}(m)]}{\sum_m \cosh[\beta\bar{H}(m)]},$$

(B4)

where $\bar{H}(m)=\sqrt{(hm+V_0M_z)^2+\Delta_0^2}$ is the total magnitude of the mean field. This equation allows us to obtain the phase diagram for any ratio of A_0/V_0, keeping $H_\perp \ll \Omega_0/\mu_B$. Near the transition line (so $M^z\ll 1$) and following Banerjee and Dattagupta,[32] we expand Eq. (B4) in M^z and obtain Eq. (26).

[1] D. Bitko, T. F. Rosenbaum, and G. Aeppli, Phys. Rev. Lett. **77**, 940 (1996).

[2] D. H. Reich, B. Ellman, J. Yang, T. F. Rosenbaum, G. Aeppli, and D. P. Belanger, Phys. Rev. B **42**, 4631 (1990).

[3] T. F. Rosenbaum, J. Phys.: Condens. Matter **8**, 9759 (1996).

[4] W. Wu, B. Ellman, T. F. Rosenbaum, G. Aeppli, and D. H. Reich,

Phys. Rev. Lett. **67**, 2076 (1991).

[5] W. Wu, D. Bitko, T. F. Rosenbaum, and G. Aeppli, Phys. Rev. Lett. **71**, 1919 (1993).

[6] J. Brooke, T. F. Rosenbaum, and G. Aeppli, Nature (London) **413**, 610 (2001).

[7] J. Brooke, D. Bitko, T. F. Rosenbaum, and G. Aeppli, Science

284, 779 (1999).

[8] S. Ghosh, R. Parthasarathy, T. F. Rosenbaum, and G. Aeppli, Science **296**, 2195 (2002).

[9] R. Giraud, W. Wernsdorfer, A. M. Tkachuk, D. Mailly, and B. Barbara, Phys. Rev. Lett. **87**, 057203 (2001).

[10] R. Giraud, A. M. Tkachuk, and B. Barbara, Phys. Rev. Lett. **91**, 257204 (2003).

[11] B. Barbara, R. Giraud, W. Wernsdorfer, D. Mailly, P. Lejay, A. Tkachuk, and H. Suzuki, J. Magn. Magn. Mater. **272-276**, 1024 (2004).

[12] M. Schechter and P. C. E. Stamp, Phys. Rev. Lett. **95**, 267208 (2005).

[13] N. V. Prokof'ev and P. C. E. Stamp, Rep. Prog. Phys. **63**, 669 (2000).

[14] H. M. Ronnow, R. Parthasarathy, J. Jensen, G. Aeppli, T. F. Rosenbaum, and D. F. McMorrow, Science **308**, 389 (2005).

[15] H. M. Ronnow, J. Jensen, R. Parthasarathy, G. Aeppli, T. F. Rosenbaum, D. F. McMorrow, and C. Kraemer, Phys. Rev. B **75**, 054426 (2007).

[16] M. Schechter and N. Laflorencie, Phys. Rev. Lett. **97**, 137204 (2006).

[17] S. Ghosh, T. F. Rosenbaum, G. Aeppli, and S. N. Coppersmith, Nature (London) **425**, 48 (2003).

[18] S. M. A. Tabei, M. J. P. Gingras, Y. J. Kao, P. Stasiak, and J. Y. Fortin, Phys. Rev. Lett. **97**, 237203 (2006).

[19] M. Schechter, P. C. E. Stamp, and N. Laflorencie, J. Phys.: Condens. Matter **19**, 145218 (2007).

[20] M. Schechter, Phys. Rev. B **77**, 020401(R) (2008).

[21] P. B. Chakraborty, P. Henelius, H. Kjonsberg, A. W. Sandvik, and S. M. Girvin, Phys. Rev. B **70**, 144411 (2004).

[22] S. Bertaina, B. Barbara, R. Giraud, B. Z. Malkin, M. V. Vanuynin, A. I. Pominov, A. L. Stolov, and A. M. Tkachuk, Phys. Rev. B **74**, 184421 (2006).

[23] N. V. Prokof'ev and P. C. E. Stamp, J. Low Temp. Phys. **104**, 143 (1996).

[24] N. V. Prokof'ev and P. C. E. Stamp, Phys. Rev. Lett. **80**, 5794 (1998).

[25] P. C. E. Stamp and I. S. Tupitsyn, Phys. Rev. B **69**, 014401 (2004).

[26] P. E. Hansen, T. Johansson, and R. Nevald, Phys. Rev. B **12**, 5315 (1975).

[27] G. Mennenga, L. J. deJongh, and W. J. Huiskamp, J. Magn. Magn. Mater. **44**, 59 (1984).

[28] G. S. Shakurov, M. V. Vanyunin, B. Z. Malkin, B. Barbara, R. Yu. Abdulsabirov, and S. L. Korableava, Appl. Magn. Reson. **28**, 251 (2005).

[29] D. M. Silevitch, D. Bitko, J. Brooke, S. Ghosh, G. Aeppli, and T. F. Rosenbaum, Nature (London) **448**, 567 (2007).

[30] S. M. A. Tabei, F. Vernay, and M. J. P. Gingras, Phys. Rev. B **77**, 014432 (2008).

[31] K. Andres, Phys. Rev. B **7**, 4295 (1973).

[32] V. Banerjee and S. Dattagupta, Phys. Rev. B **64**, 024427 (2001).

[33] A. Biltmo and P. Henelius, Phys. Rev. B **76**, 054423 (2007).

[34] M. J. Stephen and A. Aharony, J. Phys. C **14**, 1665 (1981).

[35] P. E. Jonsson, R. Mathieu, W. Wernsdorfer, A. Tkachuk, and B. Barbara, Phys. Rev. Lett. **98**, 256403 (2007).

[36] J. A. Quilliam, C. G. A. Mugford, A. Gomez, S. W. Kycia, and J. B. Kycia, Phys. Rev. Lett. **98**, 037203 (2007).

[37] B. Barbara, Phys. Rev. Lett. **99**, 177201 (2007).

[38] Y. Imry and S. K. Ma, Phys. Rev. Lett. **35**, 1399 (1975).

[39] D. S. Fisher and D. A. Huse, Phys. Rev. Lett. **56**, 1601 (1986).

[40] D. S. Fisher and D. A. Huse, Phys. Rev. B **38**, 386 (1988).

[41] C. Ancona-Torres, D. M. Silevitch, G. Aeppli, and T. F. Rosenbaum, Phys. Rev. Lett. **101**, 057201 (2008).